MAGNETIC RESONANCE SPECTROSCOPY IN UROLOGICAL ONCOLOGY

MAGNETIC RESONANCE SPECTROSCOPY IN UROLOGICAL ONCOLOGY

Een wetenschappelijke proeve op het gebied van de Medische Wetenschappen

PROEFSCHRIFT

ter verkrijging van de graad van doctor aan
de Katholieke Universiteit Nijmegen,
volgens besluit van het College van Decanen
in het openbaar te verdedigen op
dinsdag 24 mei 1994
des namiddags om 3 30 uur precies

door

Erik Bastiaan Cornel
geboren op 11 september 1964 te Harlingen

Promotor	Prof Dr F M J Debruyne
Co-promotores	Dr A Heerschap
	Dr G O N Oosterhof
	Dr J A Schalken

The investigations presented in this thesis were performed in the departments of Urology, Radiology, Biophysical Chemistry (Dutch hf-NMR facilities), Medical Statistics and the Central Animal Laboratory of the Catholic University of Nijmegen (The Netherlands)

The studies were financially supported by the Dutch Kidney Foundation (project number #C91 1105), the Siemens Company and the foundation for advancement of Urological Research (STIWU)

The publication of this book was supported by Pharmacia, Hoogland Medical b v , Stichting Urologie 1973 and the Dutch Kidney Foundation

CIP-GEGEVENS KONINKLIJKE BIBLIOTHEEK, DEN HAAG

Cornel, Erik Bastiaan

Magnetic resonance spectroscopy in urological oncology /
Erik Bastiaan Cornel. - [S.l. : s n.]
Proefschrift Nijmegen
ISBN 90-9007191-1
Trefw.. magnetische resonantie / spectroscopie / kanker.

Aan: *José*
Anna
mijn ouders

VOORWOORD

Vele mensen hebben aan de totstandkoming van dit proefschrift bijgedragen Zonder hun hulp en inzet, die ik ten zeerste heb gewaardeerd, zou het voor mij een onmogelijke opgave zijn geweest Ik wil hen daarom bij deze heel hartelijk dank zeggen

CONTENTS page

This thesis is based on the following papers

- **E.B. Cornel**, G A H J Smits, G O N Oosterhof, H F M Karthaus, F M J Debruyne, J A Schalken and A Heerschap Characterization of human prostate cancer, benign prostatic hyperplasia and normal prostate by in vitro ^{1}H and ^{31}P magnetic resonance spectroscopy *J Urol*, **150**, 2019-2024, 1993

- **E.B. Cornel**, A Heerschap, G A H J Smits, G O N Oosterhof, F M J Debruyne and J A Schalken Magnetic resonance spectroscopy detects metabolic differences between seven Dunning rat prostate tumor sublines with different biological behaviour *Prostate, in press*

- **E.B. Cornel**, G A H J Smits, J E de Ruijter, A Heerschap, G O N Oosterhof, F M J Debruyne and J A Schalken In vitro proton magnetic resonance spectroscopy of four human prostate cancer cell lines *Submitted*

- G A H J Smits, **E.B. Cornel**, E v d Boogert, G O N Oosterhof, F M J Debruyne J A Schalken and A Heerschap Effects of high energy shock waves on tumor blood flow and metabolism, $^{31}P/^{1}H/^{2}H$ nuclear magnetic resonance spectroscopic studies *Submitted*

  E.B. Cornel, G A H J Smits, A Heerschap, F M J Debruyne, J A Schalken and G O N Oosterhof The effects of successive High Energy Shock Wave administration on tumor blood flow *Submitted*

Chapter 1

INTRODUCTION

INTRODUCTION TO NUCLEAR MAGNETIC RESONANCE SPECTROSCOPY

The nuclear magnetic resonance phenomena was discovered in 1946 by Purcell and Bloch [9,129]. This technique is based on the involvement of the interaction between the magnetic moment (nuclear spin) of certain nuclei and a magnetic field [50,84]. For example, nuclei with a nuclear spin of 1/2 will have two orientations with slightly different energy levels which are proportional to the magnitude of the applied field. Transitions between these two energy levels can be induced by the application of a radiofrequency pulse. The exact frequency depends on the magnetic field and the magnetogyric ratio. Since the magnetogyric ratio varies from one isotope to another, different nuclei present in the same magnetic field will have different observation frequencies. As a consequence only one nuclear isotope can be studied at a time. Moreover, the spatial or chemical environment influences the local magnetic field, and the same nucleus in different chemical environments will give rise to resonance signals at different frequencies. As a result, at a certain field strength, each molecule will have a specific resonance pattern. Because of this unique property MRS can be used to monitor various metabolites simultaneously. Since the area under each peak is proportional to the concentration of the metabolite, absolute quantification can also be performed.

MRS metabolite studies can be performed on a number of nuclei e.g. phosphorus, hydrogen, deuterium, fluorine, carbon and nitrogen. ^{1}H and ^{31}P MRS are most commonly used in biomedical cancer research. ^{31}P MRS provides information concerning energy as well as lipid metabolism. The energy metabolism is assessed by measuring phosphocreatine, adenosine tri phosphates, inorganic phosphate and the pH whereas the lipid metabolism is monitored by the determination of phosphomono esters and phosphodiesters. ^{1}H MRS is used to monitor compounds such as amino acids, lactate, citrate, (phospho)creatine, choline containing metabolites and taurine. Deuterium MRS is used to measure (tumor) blood flow. ^{19}F MRS is currently applied to measure the absorption, distribution, metabolism and excretion of fluorinated drugs. Finally, ^{13}C and ^{15}N MRS are used in dynamic metabolic pathway studies.

THE BIOCHEMICAL BACKGROUND OF ^{1}H and ^{31}P MRS

Energy metabolism

Glycolysis is a sequence of reactions that converts glucose into pyruvate with concomitant production of ATP, occurring in the cytoplasm of the cell.

glucose + 2 Pi + 2 ADP + 2 NAD^+ → 2 pyruvate + 2 ATP + 2 NADH + 2 H^+ + 2H_2O

The end product, pyruvate, will under normal aerobic circumstances be transported to the mitochondriae where through oxidative decarboxylation acetylcoA is formed that enters the citric acid cycle (figure 1.).

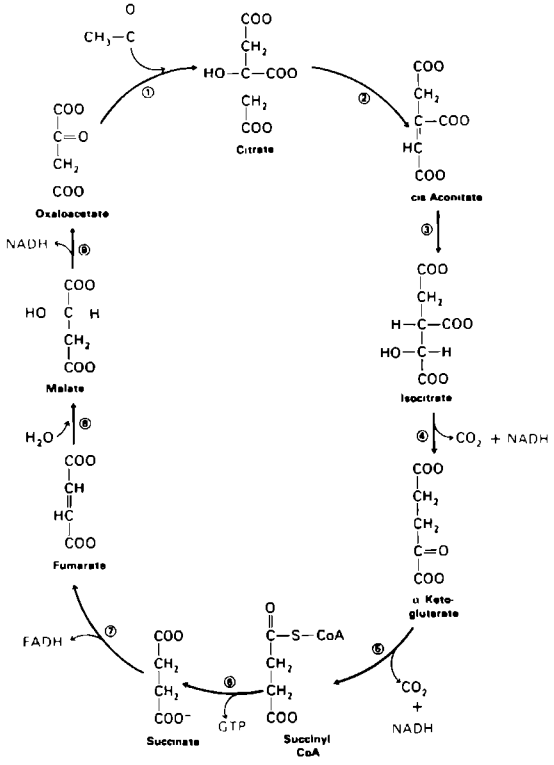

Figure 1. Citrate acid cycle Enzymes 1-9 are 1 Citrate synthetase, 2 Aconitase, 3 Aconitase, 4 Isocitrate dehydrogenase, 5 α-ketoglutarate dehydrogenase, 6 Succinyl Coa synthethase, 7 Succinyl dehydrogenase, 8 Fumarase, 9 Malate dehydrogenase (Stryer L Biochemistry page 289, Freeman and Company, New York 1981)

The citric acid cycle is the main generator of ATP. Consequently, the need for ATP regulates the rate of the citric acid cycle. Three enzymes play a key role in the control of the cycle: citrate synthetase, isocitratedehydrogenase and α-ketoglutarate dehydrogenase.

In cancer cells or under circumstances where the oxygen supply is insufficient, pyruvate will stay in the cytosol where it is converted to lactate

$$\text{pyruvate} + \text{NADH} + \text{H}^+ \rightarrow \text{lactate} + \text{NAD}^+$$

Several metabolites of the glycolysis and the citrate acid cycle can be identified in ^{1}H and ^{31}P MRS spectra Especially the ^{31}P MRS spectra provide information about the bioenergy status of the investigated sample phosphocreatine, ATP as the energy rich molecules and inorganic phosphate (Pi) as breakdown product can be accurately measured

Phospholipid metabolism

The biosynthesis of phosphatidylcholine and phosphatidylethanolamine, known as the Kennedy pathway, was elucidated in 1956[75]

$$\text{choline} \rightarrow \text{phosphocholine} \rightarrow \text{cytidine-diphosphocholine} \rightarrow \text{phosphatidylcholine}$$

This three-step pathway is catalyzed by cholinekinase, phosphocholine cytidyl-transferase, and phosphocholine transferase respectively Phosphatidylethanolamine synthesis requires three analogous steps

ethanolamine
↓
phosphoethanolamine
↓
cytidine-diphosphoethanolamine
↓
phosphatidylethanolamine

catalyzed by ethanolaminekinase, phosphoethanolamine cytidyltransferase, and phosphoethanolamine transferase respectively

The breakdown of phosphatidylcholine (or -ethanolamine) to lysophosphatidylcholine (or ethanolamine), to glycerophosphocholine (or ethanolamine), to choline (or ethanolamine) are catalyzed by the same enzymes phospholipase A, lysophospholipase, and glycerophosphorylcholine phosphodiesterase respectively

The synthesis and breakdown pathways are closely linked Ethanolamine is an inhibitor of choline kinase and of glycerophosphorylcholine phosphodiesterase, whereas choline inhibits ethanolamine kinase and also the last step towards choline and ethanolamine in the degradation pathways

In ^{31}P MRS spectra, various phosphorus containing metabolites can be monitored to obtain information about the phospholipid metabolism

INTRODUCTION TO IN VITRO MRS

In vitro MRS analyses have been performed on perfused cells[47 90], biopsy material[74 98 102 103], or extracted tissues or cells.[40 60 97 99 100] MRS of **cultured cells** has the advantage that the effects of different environmental conditions such as nutrient supply, hypoxia and pH on tumor cells can be investigated. Moreover, cell lines offer the possibility to investigate potential diagnostic and prognostic markers of certain cancers without being hampered by tissue heterogeneity. Unfortunately difficult MRS pulse programs are necessary to ensure that the cells are monitored and not the culture media.

Studying **biopsy specimens** gives us the opportunity to correlate MRS findings with histology.[74 98 102 103] Freshly excised tissues can be placed directly or after storage at -80° C for up to 6 weeks, in a MRS tube. MRS spectra can be recorded and directly afterwards the whole tissue specimen is available for histological examination. The pathological findings e.g, the presence of cancer and the percentage of the various cell types can now be correlated with the MRS metabolic pattern of the biopsy. Finally, *in vitro* MRS can be done on **extracted tissues and / or cells.**[40 60 97 99 100] The most commonly used extraction methods in cancer research are perchloric acid extraction and chloroform / methanol extraction. The former is used for the identification of small water soluble metabolites and the latter is used for lipid metabolite studies.[40 60 97 98 99] Analysis of extracted samples allows (1) an unambiguous assignment of resonances thus aiding assignment of less well-resolvedin vivo MRS spectra (fig. 2), (2) absolute quantification of metabolite concentrations and (3) facilitates the understanding of biochemical mechanisms underlying spectral modifications observed during tumor growth or response to therapy. The merits and limitations of in vitro MRS are summarized in table 1.

Table 1. Merits and limitations of in vitro MRS.

advantages	disadvantages
• High magnetic fields possible • Homogeneous samples • Highly resolved spectra • Easy to quantify • High signal to noise ratio possible	• Artifacts may be induced by sample handling

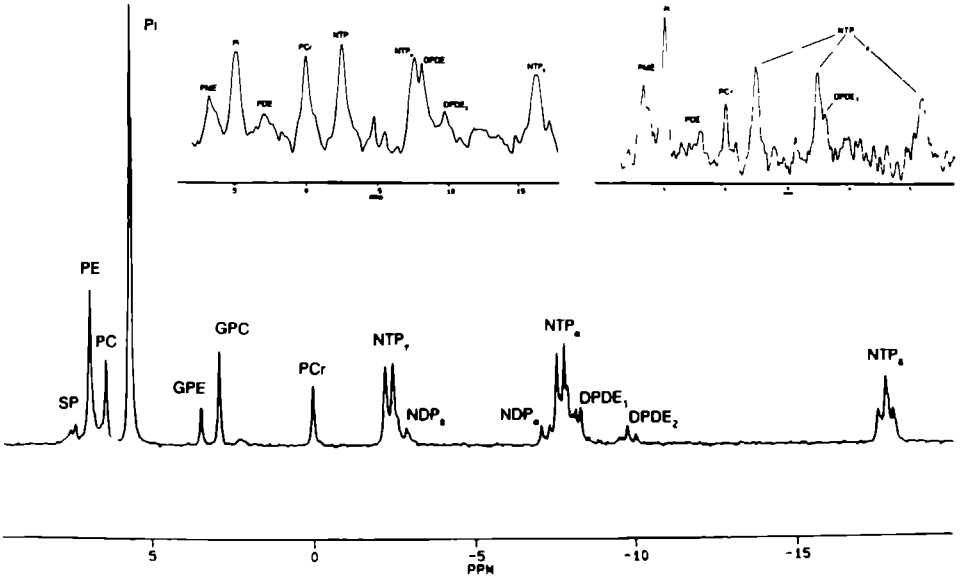

Figure 2. In vitro and in vivo 81 MHz ^{31}P NMR spectra of a control (untreated) NU-1 human kidney cancer xenograft The major peaks in the in vitro spectrum (below) are attributed as follows, SP: sugarphosphates, PME. phosphomonoesters, PE phosphoethanolamine, PC. phosphocholine, Pi· inorganic phosphate, PDE· phosphodiesters, GPE glycerophosphoethanolamine, GPC. glycerophosphocholine, PCr phosphocreatine, NTP nucleoside triphosphate, NDP nucleoside diphosphate, DPDE· diphosphodiester, $DPDE_1$ NAD (oxidized nicotinamide adenine dinucleotide, $DPDE_2$ nucleosidediphosphorylsugars
Above the in vitro NMR spectrum, two in vivo NMR spectra are shown

INTRODUCTION TO IN VIVO MRS

Genetic diseases, inflammatory processes, neoplasms, systemic metabolic and endocrine disorders have been studied with MRS.[5 51 110 115 116 130 138 172] Despite promising results obtained in *in vivo* MRS in animal studies, MRS is not routinely used in the present clinical practice. Several reasons have to be taken into account. First, the broad knowledge of the biochemistry and pathophysiology of the investigated diseases which is necessary for the interpretation of the information content available in the MRS spectra is lacking. Secondly, many technical difficulties need to be resolved in order to obtain high resolution spectra. Finally, since MRS is an expensive and relative time consuming procedure, clinical trials are needed to address its additional value for diagnosis and treatment of patients.

THE APPLICATION OF MRS IN TUMOR CELL BIOLOGY

Tumor characterization

One of the investigative goals of current MRS research in oncology is to answer the question whether MRS can detect metabolic markers / patterns specific for cancer and if so if these are of value in improving diagnosis / detection Several human malignancies have been characterized with ^{1}H, ^{31}P and ^{13}C *in vitro* MRS [2 6 35 74 98 110 119 153 154] In general, changes in the phospholipid metabolism, e g increased phosphomonoester / phosphodiester ratios were indicative for malignancies [2 6 35 74 98 119]

With respect to *in vivo* ^{1}H and ^{31}P MRS, the majority of studies have been performed in brain malignancies (review Negendank et al) [110] This is due to the fact that high resolution MR spectra can be easily obtained because large lipid resonances, that are difficult to suppress selectively, are absent in the brain ^{31}P MRS studies of human cancers outside the brain have revealed that tumors are slightly alkaline and tend to contain high levels of phosphomono- and diesters and low phosphocreatine [13 101 106 107 115 117 127 151 159] For a few malignancies originating outside the brain, special metabolic derangements have been described e g , changes in citrate metabolism for prostate cancer [106 166] Furthermore melanin has been detected as a marker for uveal melanomas [91]

Monitoring tumor therapy

Changes in the MR spectra after initiation of treatment might correlate with the efficacy of tumor treatment The effects of various therapies, e g hormonal-, radio-, chemo-, thermo-, immuno and High Energy Shock Waves (HESW) tumor therapy have been monitored by *in vivo* MRS in humans as well as in animals [42 54 55 86 87 112 137 151 152 155 161 165 169 170] Hormonal treatment of the androgen sensitive rat prostate cancer resulted in a significant decrease of PCr / NTP ratio [169] In contrast, successful endocrine therapy of rat breast cancer gave a rise in PCr and NTP peaks [137] Also for chemotherapy and radiotherapy positive and negative influences on tumor energy metabolism have been described, depending on the tumor model, dose of irradiation and dose and kind of chemotherapeutic agent [161] Hyperthermia as well as HESW exposure of human renal xenografts in nude mice resulted in a decrease in high energy phosphates, increase of inorganic phosphate and acidification of the treated tumors [112 155]

There have been a limited number of human *in vivo* MRS studies evaluating metabolite changes after therapy Changes in phospholipid metabolism, e g decreased phosphomonoesters, have been reported in patients responding to chemo- and radiotherapy [15 39 55 73 81 113 114 132 139 134]

Monitoring tumor perfusion

The efficacy of a number of therapies, e g. chemo-, radio- and thermotherapy, depends on the tumor blood flow (TBF) status [45] Hypoxic cells are not sensitive to radiotherapy, whereas poor tissue perfusion enhances the efficacy of thermotherapy.[71] The biodistribution of chemotherapeutic drugs, and thus their efficacy, also depends on perfusion.[71] TBF can also be altered by several treatments, e.g. thermotherapy and HESW.[53 112] Monitoring the TBF before and after treatment is therefore of importance in evaluating the efficacy of such TBF dependent therapies.

Several methods can be used to measure TBF and perfusion, either directly or indirectly.[3] The concept of using deuterium (D_2O) as a MRS detectable tracer in the measurement of TBF was introduced in 1978 by Ackerman et al.[1] Since then several approaches have been contrived to calculate TBF. The tracer, i.e. deuterium, can be injected i.v. or directly into the tumor. Both approaches have their advantages and disadvantages and both have proven to be sensitive and reproducible methods in the determination of TBF and perfusion.[45 78 83] Tracer detection can be done by MR spectroscopy[77] or MR imaging,[45 83 162] This non-destructive and mostly non-invasive technique allows repeated monitoring of the same subject. It is therefore an ideal technique to monitor changes in TBF after therapy.

OUTLINE OF THESIS

The application of magnetic resonance based techniques has expanded in clinical medicine in the past few years In particular, magnetic resonance imaging (MRI) has become one of the major new tools in diagnostic radiology Magnetic resonance spectroscopy (MRS) is using the same hardware as MRI but provides information at the biochemical level The clinical use of MRS however is still in its infancy In this thesis the value of MRS in the diagnosis of prostate cancer and in monitoring a new experimental cancer therapy, high energy shock waves, was determined The tissue characterization studies were performed with *in vitro* MRS on perchloric extracts, whereas the therapy monitoring studies were performed with *in vivo* MRS

The metabolic characteristics of malignant and benign human prostate tissue, obtained with ^{31}P and ^{1}H MRS, are described in chapter 2 in other to identify metabolic differences that may serve as a marker in prostate cancer In chapter 3 investigation concerning the metabolic status of different Dunning R-3327 rat prostate tumor lines and the relation to their different biological behaviour are described In chapter 4 we explore, with ^{1}H MRS, whether metabolic differences between human prostate cancer cell lines with different biological behaviour exist

In vivo ^{31}P, ^{1}H and ^{2}H MRS studies were performed to monitor the effects of HESW on tumor tissue In chapter 5 we corroborated the hypothesis that the vascular functionality is an important target of HESW by monitoring TBF and ^{1}H MRS In chapter 6 the effects of successive HESW exposures on tumor blood flow are evaluated with ^{2}H MRS The summary and the conclusions of this thesis are given in chapter 7

Chapter 2

CHARACTERIZATION OF HUMAN PROSTATE CANCER, BENIGN PROSTATIC HYPERPLASIA AND NORMAL PROSTATE BY IN VITRO ^{1}H AND ^{31}P MAGNETIC RESONANCE SPECTROSCOPY

INTRODUCTION

Prostate cancer is an increasing medical problem it is now the most common cancer in the western male population and the second leading cause of cancer related death in men [11] The approach to treatment depends on the stage of the cancer at the time of diagnosis Unfortunately, present methods for the detection of prostate malignancy (e g prostate specific antigen, transrectal ultrasonography and digital rectal examination) are inadequate to assign the precise tumor stage and to predict tumor behaviour [20] Therefore, new methods to improve prostate tumor staging are necessary
As yet, the clinical introduction of magnetic resonance imaging (MRI) did not significantly improve the detection and staging of prostate cancer [88 136] Recently transrectal probes were introduced that not only improved the quality of MRI but also made the prostate accessible to magnetic resonance spectroscopy (MRS) [105 106 147] MRS, basically employing the same instrumental set-up as for MRI, is able to monitor tissue metabolism non-invasively
^{31}P, ^{1}H and ^{13}C MRS have been used in studies that tried, both in vitro and in vivo, to associate relative levels of metabolites with benign or malignant prostate lesions [46 82 105 106 145 146 153 154 174] It has been suggested that the relative levels of the phosphorylated metabolites phosphocreatine (PCr) and phosphomonoesters (PME) can be used to discriminate malignant from benign tissue [106] Other investigators were able to measure the citrate concentration in prostatic tissue using ^{1}H MRS [46 82 145 146 174]
Moreover, Sillerud and associates demonstrated with the help of ^{13}C MRS a difference in relative levels of citrate between the normal and malignant prostate both in vitro and in vivo [153 154]
The current study was designed to characterize both ^{1}H and ^{31}P MRS spectra of benign and malignant prostate at high fields in order to substantiate these observations and to identify further differences that may serve as markers for malignancy Considering the spectral overlap occurring for spectra of whole tissue species, we decided to analyze perchloric acid (PCA) extracts in which resonances are relatively well resolved and easy to assign

MATERIALS AND METHODS

Tissues

Prostatic tissue, obtained by transurethral resection (TURP) was snap frozen in liquid nitrogen within 30 seconds after the start of resection This short ischaemia time should prevent the gross occurrence of anaerobic glycolysis and break down of high energy phosphates Samples ranged in size from 0 9 to 3 6 grams Tissue of patients with benign prostatic hyperplasia (BPH) (N=7), patients with advanced

adenocarcinoma of the prostate (N=4) and one patient with no signs of malignancy or BPH (NP) were included in this study.

Histology

Before processing the tissue samples for PCA extraction, 4 to 5 representative biopsies of one lesion (total material taken ± 0.20 grams) were taken for histological examination to confirm the diagnosis and to correlate possible differences in the proton and phosphorus spectra with the percentage of normal, BPH or cancerous tissue. Only for one prostate adenocarcinoma sample it was impossible to perform such an additional histological examination.

Preparation of PCA tissue extracts

PCA extraction was performed as described earlier by Smits et al.[155] In short, frozen tissue was weighed and pulverized at -80 ° C, transferred into an all glass homogenizer and 0.9 M PCA was added dropwise to a total of five times the weight of the tumor Complete tissue homogenization was achieved in approximately 30 minutes.

After centrifugation (12,000 g, 15', 4° C) of the tissue homogenates, the pellet was discarded and the pH of the supernatant was immediately adjusted to 7.5 with 9 M KOH. The PCA precipitate was centrifuged (12,000 g, 15', 4° C) and the supernatant was passed through a Chelex sample preparation disc (Bio-Rad Laboraties, Richmond, USA) and lyophilized. Lyophilizates were stored at - 20° C. Thirty percent of the lyophilizate was used for ^{1}H MRS and 70 % for ^{31}P MRS

Before the ^{1}H MRS measurements, the lyophilizates were carefully thawed and dissolved in 500 μl 20 mM potassiumphosphate buffer pH 7.0. If necessary the pH was adjusted to pH 6.9-7.1 Thereafter the samples were lyophilized and dissolved in 500 μl D_2O with 1.6 mM 3-(Trimethylsilyl) propionic acid-d4 sodium salt (TSP).

For the ^{31}P MRS measurements the lyophilizate was dissolved in 450 μl 0.5 mM dimethylphosphate, 20mM EDTA, 10 mM Tris, pH 7.8 in 30% D_2O.

^{31}P MRS measurements

The ^{31}P MRS spectra were acquired on a 200 MHz spectrometer (Bruker WM200) and were recorded with a standard 5 mm ^{31}P MRS high resolution probe employing a 50° flip angle and a pulse repetition time of 4 sec. WALTZ-16 low power broadband ^{1}H decoupling was used during data acquisition. The PCA extracts were analyzed under spinning conditions with a linewidth of the H_2O signal between 1 and 3 Hz. The chemical shifts were referenced with respect to the chemical shift position of the phosphocreatine resonance

The MRS data were further evaluated employing the NMR1 package (New Methods Research, INC, Last Syracuse, NY, USA) on a SUN Sparc station 330 (Sun Microsystems, INC, Mountain View, USA). FIDs were Fourier transformed and the

phase was manually corrected The ^{31}P MR spectra were semiautomati-cally fitted to Lorentzian lineshape model functions To enable comparison of different spectra, relative integrals of phosphor metabolite resonances of interest were expressed as ratio to the total integral values of all phosphates signals (TP) in the sample

^1H MRS measurements

One and two dimensional ^1H MRS spectra were acquired on a 500 MHz spectrometer (Bruker AM500) and were recorded with a standard 5 mm ^1H MRS probe One dimensional ^1H MRS spectra were recorded employing a 45° flip angle and a 7 3 sec pulse repetition time The resonance of H_2O was suppressed by low power continuous wave presaturation

The chemical shifts were referenced with respect to the chemical shift position of the TSP resonance

^1H MRS spectra were evaluated with NMR1 software FIDs were Fourier transformed after zero filling from 8 K to 32 K and Lorentzian to Gaussian transformation The phase was manually corrected and the spectra were semiautomatically fitted to Gaussian lineshape model functions To enable comparison of different spectra, relative integrals of proton metabolite resonances of interest were expressed as ratio to the total amount of the relative integral of the methyl resonance of lactate or total creatine (phosphocreatine plus creatine)

Homonuclear ^1H-^1H MRS measurements

For ^1H spectral assignments double quantum filtered correlated (DQF COSY) spectroscopy was performed using time proportional-phase incrementation with a spectral width of 6 KHz Spectra were acquired with 512 data points in the t_1 direction and 2K data points in the t_2 direction [94,176] The time domain data was zero filled and multiplied with a shifted sine-bell function before Fourier transformation

Statistical analysis

Differences in ratios of metabolites between the BPH and adenocarcinoma groups were investigated by the Kruskal-Wallis test at an experimental error rate of 0 05

RESULTS

The results of the histopathological evaluation of the specimens used for PCA extraction were compared with the pathology reports and confirmed that representative samples of the tissues were investigated All adenocarcinomas had a Gleason score of more than 8 Semiquantitative estimation of the percentage of tissue in the prostate cancers that could be evaluated showed more than 70% of tumor in two prostate

cancer samples In these two samples no signs of normal epithelial structures or BPH compounds were seen One sample of prostate cancer consisted of 60 % adenocarcinoma, no BPH and less than 5% normal epithelial structures were found One BPH sample consisted for almost 100% of glandular hyperplasia In the other six samples the percentage of BPH was 40-50% with 10-20% normal epithelial structures It must be emphasized that the number of patients with BPH and adeno-carcinoma of the prostate are small Moreover, all tumors are in an advanced stage Our results, as presented below, should therefore be considered as the first step in characterization of the metabolic content of the prostate and evaluation of the metabolic state of BPH and *advanced* prostate cancer

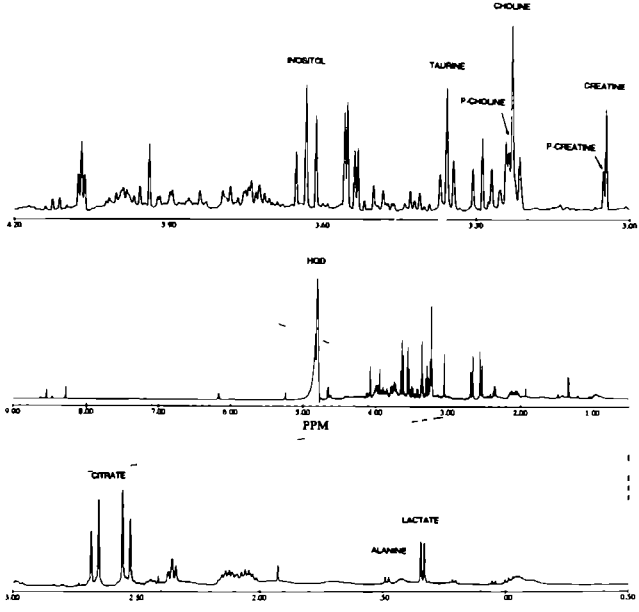

Figure 1. In vitro ^{1}H NMR spectrum with two expanded parts, of a PCA extract of normal prostatic tissue Peak assignments are indicated

^{1}H Nuclear Magnetic Resonance Spectroscopy

A 500 MHz proton MRS spectrum of a PCA extract of normal prostate tissue, with two expanded parts, is shown in figure 1 Numerous resonance peaks, originating from protons of prostate compounds can be distinguished in the spectrum Assignments for the methyl singlet peaks of phosphocholine (PC), choline (Chol) and (phospho)creatine ((P)Cr) were taken from the literature [40 124] A number of other

resonances were identified with the help of the double-quantum filtered correlated (DQF-COSY) homonuclear ^1H-^1H spectroscopy (Figure 2).

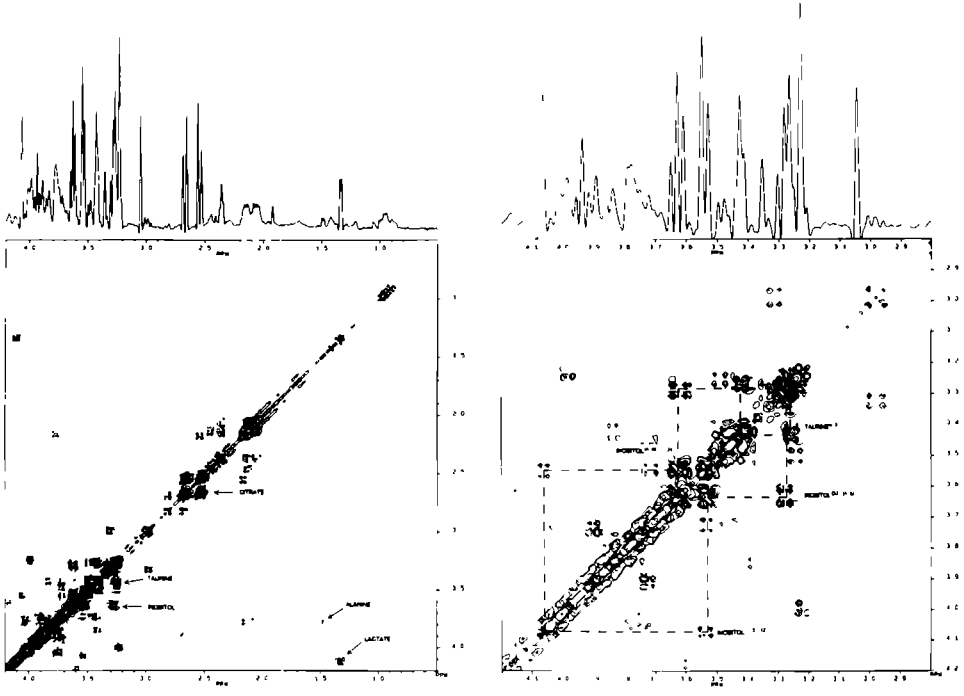

Figure 2. Double-quantum filtered correlated (DQF-COSY) homonuclear ^1H-^1H spectra (A), with one expanded part (B) of a PCA extract of normal prostatic tissue Cross peak connectivities used for assignments are indicated with arrows

In Figures 2A and 2B proton-proton connectivities are indicated in the COSY spectra used for the assignment of lactate (Lac), alanine (Ala), citrate (Cit), taurine (Tau) and inositol (Ino). Many more connectivities were observed that may serve identification of other compounds. However, for this study we have restricted ourselves to an analysis of prostate compounds contributing to the most dominating resonances in the spectrum. These resonances are also expected to be important for in vivo MRS

studies. For each compound the best resolved resonance(s) were selected for quantitation purposes. A signal of a stable homogeneous distributed compound would be ideal as an internal tissue standard for quantitation. Such a compound is not available for the prostate and we have adopted the signals of total creatine (TCr) for quantification (creatine plus phosphocreatine is relatively stable during hypoxia and prolonged ischemia), but these may differ as a function of muscular content or tumor tissue.[79 80]

Table 1. ^{1}H MRS relative peak integral ratios of prostatic human tissue.

tissue	Prost ca	(n=4)	BPH	(n=7)	NP (n=1)	p
Ala/TCr	46	(25)	24	(5)	18	$p < 0.05$
Cit/Lac	15	(18)	154	(36)	308	$p < 0.05$
Cit/TCr	56	(82)	182	(108)	263	ns
Cit/TChol	106	(161)	759	(408)	209	$p < 0.05$
Chol/TCr	65	(39)	25	(6)	39	$p < 0.05$
PC/TCr	67	(31)	18	(5)	25	$p < 0.05$
Tau/TCr	512	(368)	197	(13)	291	ns
Ino/TCr	574	(175)	649	(57)	704	ns

Relative integrals of peak area's of metabolites of interest are listed as ratios to lactate or total creatine The ratios of metabolites of interest are listed as mean with standard deviation between brackets P values relate to a comparison between prostate adenocarcinoma and BPH

Table 1 lists relative peak area integral ratios involving the doublet of the CH3 group of **lactate** at 1 33 ppm, the doublet of the CH3 group of **alanine** at 1.49 ppm, the quartet of the CH2 group of **citrate** at 2.54 ppm, the singlet of the CH3 groups of **(phospho)creatine** at 3.04/3 05 ppm), the singlets of the CH3 group of **phosphocholine** and **choline** at 3.23 and 3.22 ppm respectively, the triplet of the CH2 group of **taurine** 3.42 ppm and the triplet of the CH group of **inositol** at 3.63 ppm.
In figure 3 representative ^{1}H MRS spectra are shown of PCA extracts of NP (C), BPH (B) and prostate cancer tissue (A) ^{1}H MRS spectra of BPH and the NP tissue PCA extracts were comparable for most ratios whereas the ^{1}H MRS spectra of BPH showed marked differences in the relative peak ratios as compared to the ^{1}H MRS spectra of the prostate adenocarcinomas. Most striking is the presence of citrate in the spectra of the BPH specimens and the very low or undetectable levels in the specimens of advanced prostate carcinoma (table 1. $p < 0\ 05$) In one of the two cases where citrate could be detected, normal epithelial structures were seen. In contrast, no citrate

was observed in the prostate carcinoma biopsies containing no normal epithelial structures. In addition, a significant difference of the Ala / TCr, PC / TCr and Chol / TCr ratios between BPH and prostate cancer samples was observed (table 1., $p < 0.05$).

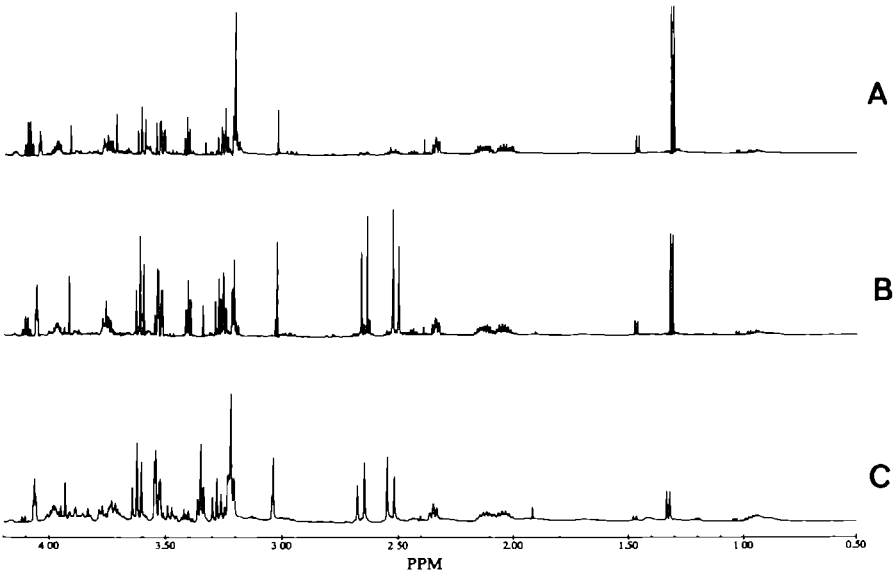

Figure 3. Representative in vitro ^{1}H MRS spectra of PCA extract of adenocarcinoma of the prostate (A), benign prostatic hyperplasia (B) and normal prostatic tissue (C)

^{31}P Magnetic Resonance Spectroscopy

Figure 4 shows a ^{31}P MRS spectrum of a PCA extract of normal prostate tissue. ^{31}P MRS resonances were assigned to phosphorylated compounds based on literature data.[14 57] Several phosphomonoester peaks, e.g. phosphoethanolamine (PE) and phosphocholine (PC), and phosphodiester peaks, e.g glycerophospho-ethanolamine (GPE) and glycerophosphocholine (GPC), as well as α, ß, and γ signals from different nucleoside triphosphate (NTP) peaks and inorganic phosphate (P_i) and phosphocreatine were identified and are indicated in figure 4. In table 2 ratios of phosphor metabolites compared to resonance integrals of total phosphate in the ^{31}P MRS spectra of the samples are presented. In figure 5 representative ^{31}P MRS spectra are shown of PCA extracts of NP (C), BPH (B) and prostate cancer tissue (A). As for the ^{1}H MRS spectra, the ^{31}P MRS spectra of BPH specimens were comparable to the ^{31}P spectrum of the NP sample. The significantly increased PC / TCr ratio in the

prostate cancer samples observed in the ^{1}H spectra was also reflected in the ^{31}P spectra where the PC / TP was significantly higher in adenocarcinoma specimens of the prostate as compared to BPH (Table 2 , $P < 0.01$) Also the GPE / TP ratio was significantly higher in the adenocarcinoma samples as compared to the BPH (Table 2 , $P < 0.05$) In contrast, the relative level of the other main phospholipid PE, was significantly lower in adenocarcinoma of the prostate as compared to BPH (Table 2 , $P < 0.05$)

Table 2. ^{31}P MRS relative peak integral ratios of prostatic human tissue

tissue	Prost Ca	(n=4)	BPH	(n=7)	NP (n=1)	p
PE/TP	127	(43)	186	(30)	162	$p < 0.05$
PC/TP	63	(16)	38	(4)	38	$p < 0.05$
PI/TP	342	(80)	282	(87)	223	ns
GPE/TP	37	(20)	11	(5)	9	$p < 0.05$
GPC/TP	25	(16)	12	(3)	9	ns
PCr/TP	21	(26)	43	(17)	39	ns

Relative integrals of peak area s of metabolites of interest are listed as ratios to the total phosphate content (TP) The ratios of metabolites of interest are listed as mean with standard deviation between brackets P values relate to a comparison between prostate adenocarcinoma and BPH

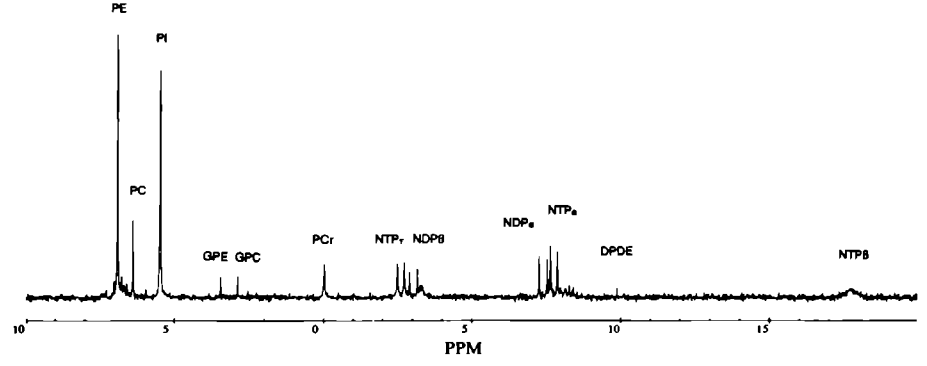

Figure 4. In vitro ^{31}P NMR spectrum of a PCA extract of normal prostatic tissue Peak assignments are indicated

DISCUSSION

The first aim of this study was to characterize the metabolic content of human prostate specimens by ^{1}H and ^{31}P MRS Thereafter we investigated whether differences in relative levels of metabolites in the ^{1}H and ^{31}P MRS spectra could distinguish between different prostate pathologies i e , between BPH and adenocarcinoma of the prostate We have chosen for an in vitro MRS study of PCA extracts of representative tissue samples thereby assuring proper detection and quantification of tissue metabolites Relative little tissue is needed to acquire an adequate signal / noise ratio and we assume that our results are well approximated reflections of the in vivo conditions because only transurethral resection material with a total ischemia time of less than 30 seconds was included in this study In comparison to most other in vitro studies the sampling of the specimens was substantially shortened avoiding possible sampling artifacts, due to degradation of metabolites and ischemia [46 82 174]

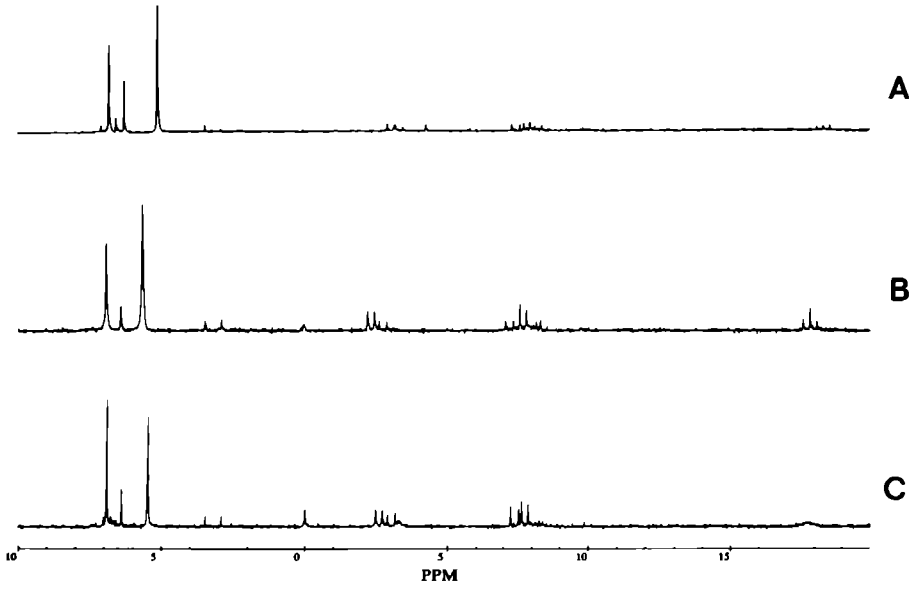

Figure 5. Representative in vitro ^{31}P MRS spectra of PCA extracts of adeno carcinoma of the prostate (A) benign prostatic hyperplasia (B) and normal prostatic tissue (C)

^{1}H- and ^{31}P are the most used nuclei in in vivo MRS practice The use of ^{1}H MRS seems most favourable because it has a much higher relative sensitivity compared with ^{31}P MRS However, the large number of proton containing metabolites may result in complex spectra, whereas ^{31}P MRS spectra are relatively easy to acquire and interpret

Finally, ^{1}H MRS provides information about proton containing compounds such as organic acids, amino acids and sugars whereas ^{31}P MRS finds its application in studies about high energy phosphate and phospholipid metabolism

For most metabolite signal ratios evaluated in this study the ^{1}H and ^{31}P MRS spectra of the single NP specimen and the BPH samples were comparable In contrast several striking differences were observed between the MRS spectra of BPH and adenocarcinoma specimens of the prostate The Cit / Lac and Cit / total choline ratios were found to be potential markers in the discrimination of benign and malignant prostatic tissue ($p < 0.05$) These ratios may be used in in vivo MRS of the prostate because the corresponding metabolite signals can be easily identified in these spectra (A Heerschap, unpublished data) Our MRS results, with respect to citrate and lactate, are in accordance with those obtained by others employing different techniques [21,30,93] Similar observations for citrate were made by Fowler et al , employing ^{1}H MRS, on the basis of other ratios [46] Recently, Kurhanewicz et al demonstrated that the citrate concentration of prostate adenocarcinomas was ten fold lower relative to normal and benign hyperplastic prostatic tissues [82]

It is assumed that in the normal prostate epithelial cells little citrate oxidation occurs and that the high level of cytosolic citrate inhibits glycolysis at the pyruvate phosphokinase step [7] Costello et al postulated that the oxidation of citrate is increased in prostate cancer cells resulting in a decreased cellular citrate concentration and increased glycolysis [7] This hypothesis fits well with our observation that the Cit / Lac ratio was significantly decreased in the prostate cancer samples as compared to BPH Moreover our results support the early notion of Cooper et al that the Lac / Cit ratio may be used to discriminate malignant from benign prostatic tissue [71]

Our results suggest a correlation between the relative amount of citrate and the percentage of *normal* epithelial structures seen in the PCA extracted specimens In cancer samples devoid of non-malignant epithelial structures no citrate could be detected by ^{1}H MRS whereas the cancer sample with 5% normal epithelial structures showed the highest relative level of citrate of all samples The effect of tissue heterogeneity on citrate levels has also been observed by Schlieber et al but for adenocarcinoma changes in the low percentage of glands did not have a major effect on citrate levels [145]

In the prostate cancer specimens the relative amounts of PC, Chol, and GPE, all cell membrane components, were significantly increased as compared to BPH All our patients had a high stage / grade of prostate cancer which have higher proliferation rates than surrounding normal tissues The increase of these metabolites may therefore be associated with an increase in membrane synthesis [22,32,142]

The relative level of PE was significantly lower for the prostate cancer samples For other cancers it has been suggested that an increase of the PE / PC ratio could serve as a marker for malignancy [74,78] However, the decreased PE / PC ratio that we

observed illustrates that this is not a general phenomenon [142] Daly et al showed that the PC content of cancer cells growing in choline enriched medium will increase with concurrent increase of GPC and GPE [32] Moreover, choline can inhibit ethanolaminokinase, and thus blocking the PE producing step, if a sufficient intracellular concentration can be reached [32] Our observations of a relative increase of PC and GPE and decrease of PE fits well with the proposed pathway

In conclusion, we characterized the major metabolic components of prostate tissue employing proton and phosphorus MRS Significant differences in the metabolic state of BPH and prostate cancers were found

Several metabolic ratios, e g Cit / Lac, Cit / TChol, PC / TCr and Chol / TCr seemed to be potential markers to differentiate prostate cancer from BPH and these may be useful in the evaluation of in vivo MRS spectra of the prostate In our ongoing in vivo MRS study of the prostate, using transrectal coils, the Cit / TChol ratio indeed seems to be useful in discriminating BPH from adenocarcinoma of the prostate [62] Whether MRS spectroscopy can aid in the diagnosis and in therapy-monitoring of prostate cancer patients remains to be investigated [107]

MAGNETIC RESONANCE SPECTROSCOPY DETECTS METABOLIC DIFFERENCES BETWEEN SEVEN DUNNING RAT PROSTATE TUMOR SUBLINES WITH DIFFERENT BIOLOGICAL BEHAVIOUR.

INTRODUCTION

With an estimated death rate of 34.000 cases in the USA in 1992, prostate cancer ranks second among cancer related deaths in males after lung cancer.[11] Moreover, prostate cancer has become the most diagnosed malignancy in USA males in 1992.[11] Unknown natural history, variable pathology and biological behaviour make prostate cancer difficult to classify into diagnostic and prognostic categories. Patients diagnosed with prostate cancer can be cured if the disease is at an early stage, i e patients with localized lesions can be cured by radical prostatectomy or radiotherapy. However, many patients will show clinical progression to metastatic disease. These are the patients that may benefit from aggressive treatments while in other patients, where the tumor will remain localized, no or less aggressive therapy may be given. Therefore, new diagnostic methods able to predict more accurately the biological behaviour of the tumor are needed since these may lead to a better base for individual treatment.

One approach to solve this problem is to investigate whether the metabolic profiles of prostate cancers differ significantly with respect to several tumor biological characteristics Magnetic resonance spectroscopy (MRS) has been introduced for non-invasive metabolic studies of cancer cells and for in vivo studies of tumors in animals and humans. For several cancers, it has been investigated whether MRS can be used to characterize differentiation grade, metastatic capacity, multi-drug resistance and hormonal dependency.[18 21 24 32 40 46 52 74 98 153 154 169 174] For prostate cancer there is still a paucity of knowledge to what extent tumors differ in their biochemical state. Vigneron and associates demonstrated that the phosphocreatine / adenosinetriphosphate ratio was significantly decreased in one hormone dependent Dunning subline compared to a hormone insensitive one.[169] It has been suggested that the relative amount of citrate in the human prostate decreases in cancer tissue related to tumor differentiation.[153] However, a recent in vitro ^{1}H MRS study of extracts of surgical specimens by Fowler and coworkers did not show any correlation between Gleason grade and citrate.[46]

The current study was designed to characterize the metabolic state of seven different Dunning R-3327 rat prostate tumor sublines employing both ^{31}P and ^{1}H MRS. We have chosen the Dunning tumor model system because the sublines differ widely in their histology, growth rate, androgen sensitivity and metastatic capacity, and therefore constitutes an appropriate tumor model system to test the hypothesis that differences in the metabolic content of sublines can be related to their different tumor biological potential. Considering the complexity that can be expected for in vivo spectra, we decided to start with an analysis of in vitro perchloric acid (PCA) extracts of the Dunning tumors. In this way assignments of resonances in the spectra are facilitated and potential differences may be revealed more easily.

MATERIALS AND METHODS

Animals

Adult male F1 hybrid rats (F344CopF1/OLA/HSD, Copenhagen male and Fisher female) were purchased from Harlan OLAC, Bicester, England The Fisher-Copenhagen rats were housed three animals per cage and subjected to a 12 hours cycle light / darkness They were provided with a standard pelleted diet (Hope Farms, Woerden The Netherlands) and acidified water (pH 3) ad libitum

Tumor Lines

Six well-characterized sublines of the Dunning R-3327 tumor were kindly provided by Dr J T Isaacs (Johns Hopkins Oncology Center, Baltimore, USA) [70] The AT-6 subline was established in our own laboratory [16] The characteristics of the H-, PIF-, PAP , G , AT-2-, AT-6 and MatLyLu sublines(MLL) are summarized in table 1 The tumors were transplanted subcutaneously in the flank of Fisher-Copenhagen rats as trocar pieces Tumors were allowed to grow to a tumor volume of 1000-1500 mm^3 Two different passages (except for the H subline) of each subline were investigated

Table 1. In vivo biological characteristics of Dunning R-3327 rat prostate cancer

Dunning Subline	Histology	Growth rate (Doubling time in days	Androgen responsive	Metas Ability
H	Well diff	22 0 ± 5 0	Yes	Low
PAP	Well diff	10 5 ± 2 0	Yes	Low
PIF	Poorly diff	3 7 ± 1 1	No	Low
G	Anaplastic	4 0 ± 0 2	Yes	Low
AT-2	Anaplastic	2 5 ± 0 2	No	Moderate
AT-6	Anaplastic	4 0 ± 1 0	No	High
MLL	Anaplastic	1 5 ± 0 1	No	High

Preparation of PCA tissue extracts

PCA extraction was performed as described earlier by Smits et al [155] In short, frozen tissue was weighed and pulverized at 80 ° C, transferred into an all glass homogenizer and 0 9 M PCA was added dropwise to a total of five times the weight of the tumor sample Complete tissue homogenization was achieved in approximately 30 minutes

After centrifugation (12,000 g, 15', 4° C) of the tissue homogenates, the pellet was discarded and the pH of the supernatant was immediately adjusted to 7 5 with 9 M

KOH. The PCA precipitate was centrifuged (12,000 g, 15', 4° C) and the supernatant was passed through a Chelex sample preparation disc (Bio-Rad Laboraties, Richmond, USA) and lyophilized. Lyophilizates were stored at - 20° C. Thirty percent of the lyophilizate was used for ^{1}H MRS and 70 % for ^{31}P MRS.
Before the ^{1}H MRS measurements, the lyophilizates were carefully thawed and dissolved in 500 μl 20 mM potassiumphosphate buffer pH 7.0. If necessary the pH was adjusted to pH 6.9-7.1 Thereafter the samples were lyophilized and dissolved in 500 μl D_2O with 1.6 mM 3-(Trimethylsilyl) propionic acid-d4 sodium salt (TSP).
For the ^{31}P MRS measurements the lyophilizate was dissolved in 450 μl 0.5 mM dimethylphosphate, 20mM EDTA, 10 mM Tris, pH 7 8 in 30% D_2O.

^{31}P MRS measurements

The ^{31}P MRS spectra were acquired on a 200 MHz spectrometer (Bruker WM200) and were recorded with a standard 5 mm ^{31}P MRS high resolution probe employing a 50° flip angle and a pulse repetition time of 4 sec. WALTZ-16 low power broadband ^{1}H decoupling was used during data acquisition. The PCA extracts were analyzed under spinning conditions with a linewidth of the H_2O signal between 1 and 3 Hz. The chemical shifts were referenced with respect to the chemical shift position of the phosphocreatine resonance.
The MRS data were further evaluated employing the NMR1 package (New Methods Research, INC, Last Syracuse, NY, USA) on a SUN Sparc station 330 (Sun Microsystems, INC, Mountain View, USA). FIDs were Fourier transformed and the phase was manually corrected. The ^{31}P MR spectra were semiautomati-cally fitted to Lorentzian lineshape model functions. To enable comparison of different spectra, relative integrals of phosphor metabolite resonances of interest were expressed as ratio to the total integral values of all phosphate signals (TP) in the sample.

1H MRS measurements

^{1}H MRS spectra were acquired on a 500 MHz spectrometer (Bruker AM500) and were recorded with a standard 5 mm ^{1}H MRS probe, employing a 45° flip angle and a 7.3 pulse repetition time. The resonance of H_2O was suppressed by low power continuous wave presaturation.
The chemical shifts were referenced with respect to the chemical shift position of the TSP resonance. ^{1}H MRS spectra were evaluated with NMR1 software. FIDs were Fourier transformed after zero-filling from 8 K to 32 K and Lorentzian to Gaussian transformation. The phase was manually corrected and the spectra were semiautomatically fitted to Gaussian lineshape model functions. To enable comparison of different spectra, relative integrals of proton metabolite resonances of interest were expressed as ratio to the total amount of the relative integral of total creatine TCr (this consists of creatine and phosphocreatine). Total creatine levels appear relatively stable

during hypoxia and prolonged ischemia[79,80], but may differ as a function of muscular content or tumor tissue in the biopsy

Statistical analysis

Differences in ratios of metabolites between the well and moderately differentiated tumors (N=6) and poorly differentiated and anaplastic (N=8), the non-metastatic (N=8) and metastatic (N=6) sublines, and the hormone dependent (N=6) and hormone independent (N=8) sublines groups were investigated by the Kruskal-Wallis test at an experimental error rate of 0 05

RESULTS

MR spectra of PCA extracts of seven Dunning R-3327 sublines were recorded and for each subline, except for the H tumor, two different passages were investigated
For correlative studies between metabolic profiles and tumor biological characteristics, the sublines were grouped according to histology, metastatic capacity or androgen responsiveness It must be emphasized that these groups are partly overlapping, e g well and moderately differentiated (H, PAP and PIF) versus poorly differentiated and anaplastic (G, AT 2, AT-6 and MLL), metastatic (AT-2, AT-6 and MLL) versus non-metastatic (H, PAP, PIF and G) whereas hormonal responsive versus hormonal non-responsive were H, PAP and G versus PIF, AT-2, AT-6 and MLL

^{31}P magnetic resonance spectroscopy

Figure 1 shows ^{31}P MRS spectra of extracts of the H and MLL Dunning tumor sublines Resonances in the spectra were assigned to the phosphomonoesters, phosphoethanolamine (PE) and phosphocholine (PC), which primarily function as precursors of phospholipid biosynthesis and to the phosphodiesters, glycero-phosphorylglycerol (GPG), glycerophosphoethanolamine (GPE) and glycero-phosphocholine (GPC), which are phospholipid catabolites [32] Not only these phosphomono and phosphodiester resonances but also cyclic sugar phosphates (C-sp), inorganic phosphate (Pi), PCr as well as alpha, beta and gamma signals from different nucleoside tri phosphate (NTP) peaks could be identified using literature data [14,57] Ratios of phosphor metabolites were obtained of ^{31}P MR spectra from all sublines investigated

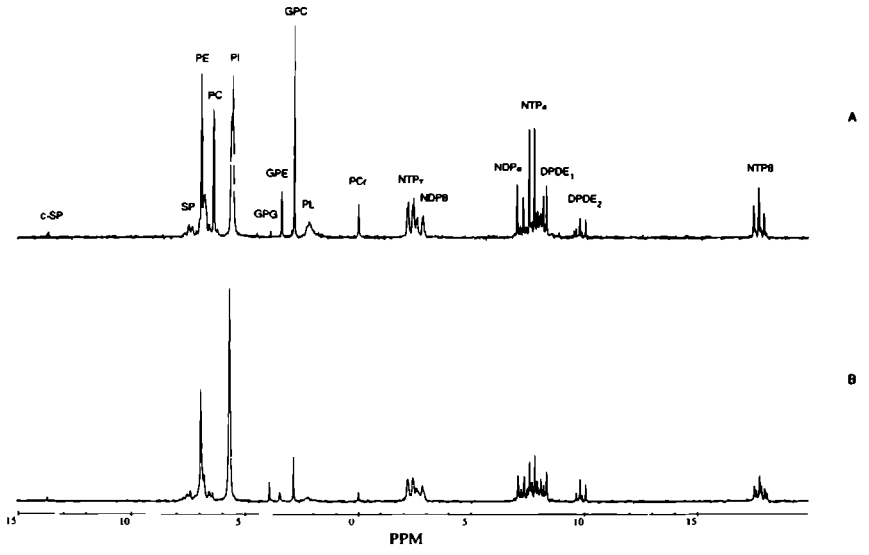

Figure 1. In vitro ^{31}P MR spectrum with peak assignments of PCA extract of parental H Dunning R-3327 tumor (A) and MatLyLu Dunning R-3327 tumor (B)

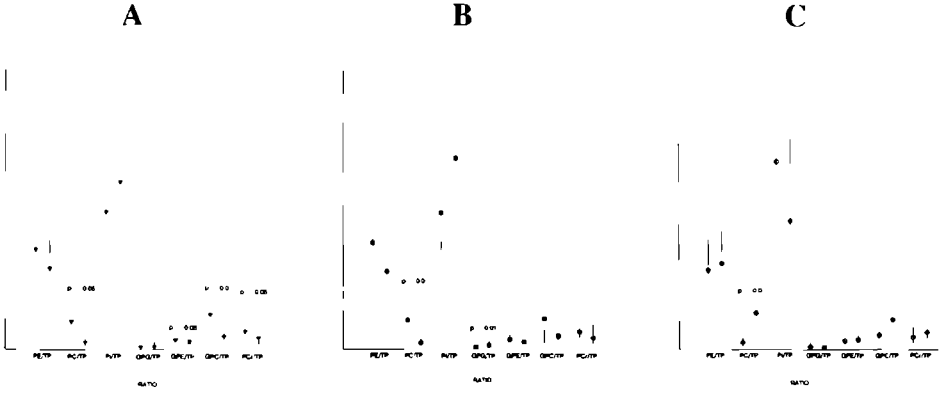

Figure 2. Ratios of integrals of ^{31}P MRS metabolites for **A** well to moderately differentiated Dunning tumor sublines (open triangle) compared with poorly differentiated or anaplastic sublines (closed triangle) **B:** metastatic (closed square) versus non metastatic (open square) sublines and **C** androgen responsive (closed circle) versus non responsive (open circle) Values are median with range (min and max value)

Several of these ratios obtained for the well and moderately differentiated sublines (H, PAP and PIF) differed from the poorly differentiated and anaplastic sublines (G, AT-2, AT-6 and MLL) The PC, GPE, GPC and PCr ratios were significantly higher for the well and moderately differentiated lines (Fig 2A) The PC / TP ratio was also significantly increased when the low metastatic sublines H, PAP, PIF and G were compared to the moderately and highly metastatic AT-2, AT-6 and MLL (Fig. 2B). All metastatic Dunning sublines contained GPG. The GPG resonance peak was also seen in the parental H subline, but at much lower relative intensity (Fig 1) With respect to androgen responsiveness, the PC / TP ratio was significantly decreased in the androgen non-responsive PIF, AT-2, AT-6, and MLL sublines (Fig 2C)

1H magnetic resonance spectroscopy

A 500 MHz proton NMR spectrum of a PCA extract of the H and MLL sublines, with two expanded parts, is shown in figures 3 and 4 respectively Numerous resonances can be distinguished in the spectrum In part, these resonances could be identified with data from the literature [25,40,124] For each compound investigated in this study the best resolved resonance(s) were selected for quantitation

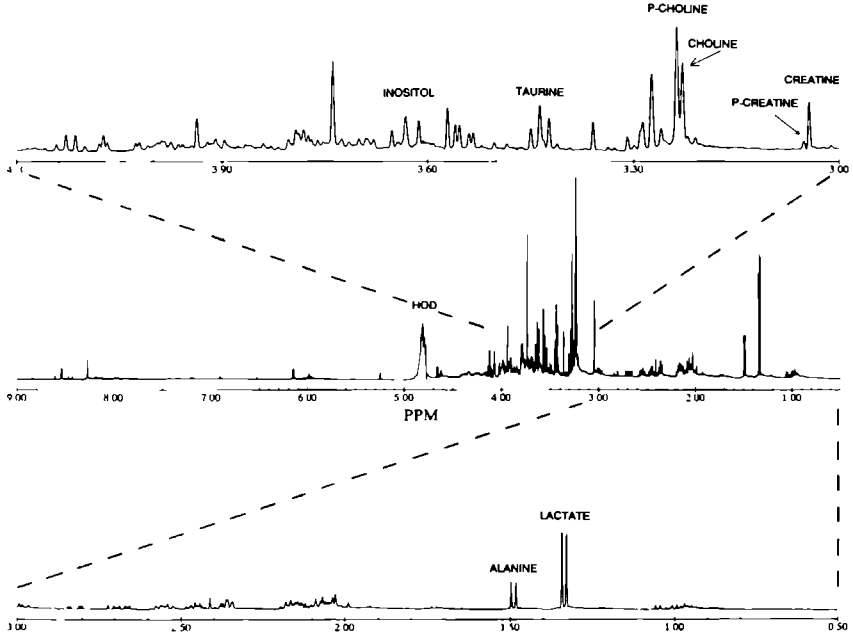

Figure 3. In vitro ^{1}H MR spectrum with peak assignments of PCA extract of parental H Dunning R-3327 tumor

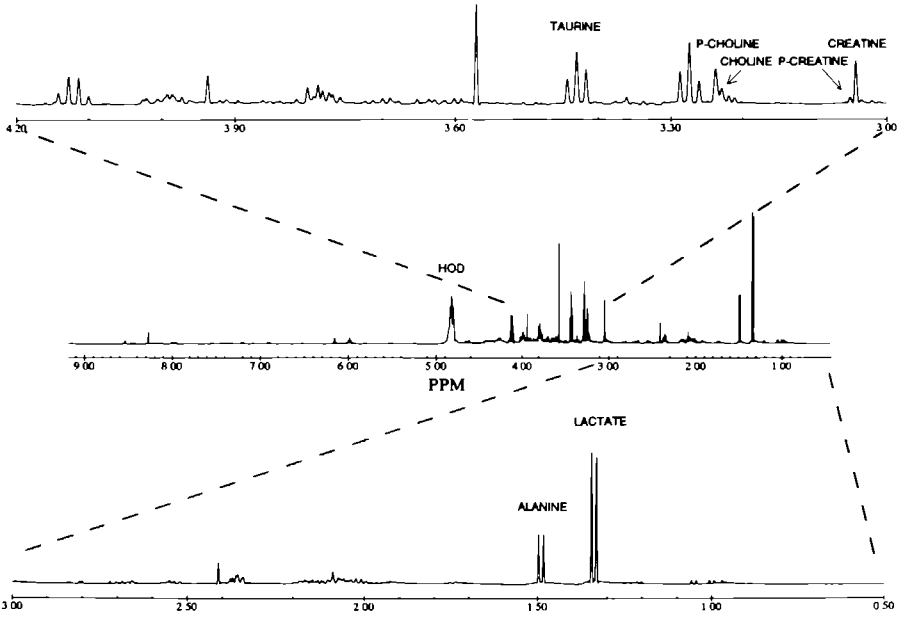

Figure 4. In vitro ^{1}H MR spectrum of PCA extract of MatLyLu Dunning R-3327 tumor

Relative peak area integral ratios involving the doublet of the CH3 group of **lactate** (Lac) at 1.33 ppm, doublet of the CH3 group of **alanine** (Ala) at 1.49 ppm, quartet of the CH2 group of **citrate** (Cit) at 2.54 ppm, singlet of the CH3 group of **(phospho)creatine** at 3.04 / 3.05 ppm), singlets of the CH3 group of **phosphocholine** (PC) and **choline** (Chol) at 3.23 and 3.22 ppm respectively, triplet of the CH2 group of **taurine** (Tau) 3.42 ppm and triplet of the CH group of **inositol** (Ino) at 3.63 ppm. The PC resonance may also contain a contribution of GPC protons.

Remarkably, inositol could only be detected in the well and moderately differentiated sublines H, PAP and PIF, but not in the poorly differentiated and anaplastic sublines G, AT-2, AT-6 and MLL (Fig. 5A). The Ino / TCr ratio was not only significantly increased when the well and moderately sublines were compared with the poorly differentiated and anaplastic ones but also the non-metastatic sublines H, PAP, PIF and G differed from the metastatic sublines regarding the Ino / TCr ratio (Fig. 5B and 5C). The significantly increased relative PC levels of the well or moderately differentiated, non-metastatic and androgen dependent sublines with respect to the poorly differentiated or anaplastic, metastatic and androgen independent sublines observed in the ^{31}P spectra (see above) was also observed in the ^{1}H MR spectra, i.e. the PC/TCr ratio was significantly higher for the same groups of sublines (Fig. 5A-C).

This was also found for the total choline (choline + phosphocholine) ratio For as well the PC / TCr as the Tchol / TCr ratio a significantly increase was found ($p < 0.05$ for TChol / TCr for all groups, results not shown) Citrate resonances were absent or extreme low in the ^{1}H MR spectra of all Dunning sublines investigated ^{1}H MR spectra of extracts of normal prostate of Fisher-Copenhagen rats does contain signals for citrate (results not shown)

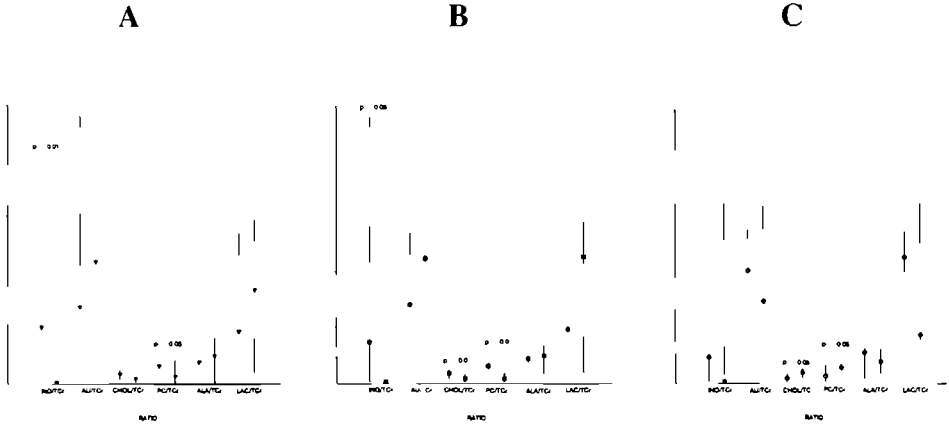

Figure 5. Ratios of integrals of ^{1}H MRS metabolites for **A** well to moderately differentiated Dunning tumor sublines (open triangle) compared with poorly differentiated or anaplastic sublines (closed triangle) **B:** metastatic (closed square) versus non-metastatic (open square) sublines and **C** androgen responsive (closed circle) versus non responsive (open circle) Values are median with range (min and max value)

DISCUSSION

Tumors of the seven Dunning sublines used in this study range from well differentiated to anaplastic are androgen dependent or independent and differ in their metastatic ability (table 1) The aim of this investigation was to characterize the metabolic profile of these Dunning R 3327 rat prostate cancer sublines as viewed by ^{1}H and ^{31}P MRS Thus we wanted to identify variations in their biochemical content which might be related to differences in biological behaviour By analyzing PCA extracts, several well resolved resonances were identified which gave us the opportunity to quantify some main biochemical components in rat prostatic cancer tissue

The main metabolites detected with ^{31}P and ^{1}H MRS in the Dunning tumors were similar to those observed in our earlier study in which human prostate samples were investigated.[25] Several metabolic ratios appeared to be valuable for the evaluation of sublines clustered for one specific biological characteristic.

Differentiation grade

The relative levels of phosphocholine, glycerophosphocholine and glycerophosphoethanolamine were found to discriminate between well (or moderately) differentiated and anaplastic or poorly differentiated tumor sublines. As phosphocholine levels also correlated with metastatic potential and androgen insensitivity, this marker is not specific for differentiation alone. The for in vivo MRS more important relative level of total choline (choline + phosphocholine) was also increased for these three biological characteristics. Thus these markers may be useful to identify an aggressive subpopulation of prostate cancer tumor cells.

A relation between differentiation grade and phospholipid metabolism has been suggested for several other tumors.[2,18,52] Agris and Campbell showed with the help of ^{1}H NMR an enhanced accumulation of PC during dimethylsulfoxide induced differentiation of Friend Leukaemia cells.[2] In the same model Carpinelli et al. found with ^{31}P MRS an increase in PC and a concomitant decrease of GPC and GPE levels.[18] Galons and associates used a human colon adenocarcinoma model and also showed with ^{31}P and ^{1}H MRS high levels of PC and choline after inducing differentiation.[52] These observations together with our findings clearly demonstrate that alterations in the phospholipid metabolism plays a role in the process of differentiation although changes may occur at different levels in the phospholipid metabolism for tumors of different origin. An increased PC content may have several different causes: increased phospholipid synthesis, enhancement of phosphokinase activity, inhibition of the cytidylyltransferase activity or an increment in the pool of intracellular choline.[18] Further alterations in the phospholipid metabolism found in the Dunning tumor model system may be explained by the fact that increased PC content leads to a increase of GPE and GPC due to inhibition of GPE diesterase.[4,32]

The well differentiated H- and PAP sublines and the moderately differentiated PIF subline contain high levels of inositol, whereas this compound was not detectable in the other sublines. Apparently inositol metabolism in the anaplastic rat prostate tumors differs substantially from that in the well differentiated prostate tumors.

The biochemical role of inositol is not well known.[140] It is a requirement for the growth of mammalian cells. It may be a "storage" form for phosphorylated inositols, of which some have a function as intracellular messengers, or for glucose and in addition may have a role as an osmoregulator. As yet it is unclear why the content of inositol in non-differentiated tumor cells is reduced. Any of its potential functions may be involved.

The relative content of PCr also correlated with differentiation grade. The reduced

PCr levels for the anaplastic and poorly differentiated sublines are indicative for a poorer high energy phosphate metabolism Previously, the relative amount of PCr has been indicated as a marker for the hormonal dependency of the several tumors [137 169]

Metastatic ability

^{31}P MR spectra of the highly metastatic MLL and AT-6 sublines and the moderately metastatic AT-2 subline showed a small but significant peak at 3 9 ppm We have assigned this peak to GPG which is probably a degradation compound of a phospholipid produced by a phospholipase A [14] GPG may be a marker for metastatic capacity however this peak was also found in one of the slowly growing, low-metastatic parental H tumors

Due to the overlap of groups also the Ino / TCr ratio appeared to be significantly different in the non-metastatic sublines versus the metastatic ones, but regarding the very strong relation with histology the specificity of this finding is questionable Although, as for choline and phosphocholine, inositol can be a potential general marker for an aggressive subpopulation of prostate cancer cells

Androgen responsiveness

Several studies have suggested that ^{31}P MRS can be helpful in distinguishing hormone sensitive from hormone insensitive cancers [137 169] In particular an increased PCr / ATP ratio was found in a hormone sensitive Dunning tumor subline when compared to a hormone insensitive tumorline [169] Androgen deprivation (orchiectomy) resulted in a significant decrease in the PCr / ATP ratio In this in vivo study only one subline with this particular tumor biological characteristic was investigated In the present in vitro study, three different hormone sensitive and four different hormone insensitive sublines were investigated and no specific correlation for hormonal sensitivity with the metabolites examined in this study could be made neither by ^{31}P - nor by ^{1}H MRS Only the two PAP tumors showed a higher PCr / TP ratio then hormone insensitive sublines but for the other two hormone sensitive lines the same increase was not observed

Citrate levels

Previous studies have observed very low or undetectable levels of citrate in prostate cancer tissue / cells compared to benign prostatic hyperplasia, probably due to an altered citrate metabolism [25 49 82 145] In the present study we could not detect citrate signals in the spectra of the Dunning sublines which may seem to fit well with these findings for human prostate tissue However, the original parental H tumor was derived from the dorsal prostate of the rat which does not contain citrate producing glands [31 158] Therefore the absence of citrate in all Dunning tumors is not surprising and in these cases not indicative for prostate cancer tissue

Conclusions

The present findings show that in the Dunning R-3327 tumor model, well differentiated, non metastatic and hormone dependent tumors can be distinguished from anaplastic or poorly differentiated, metastatic and hormone independent tumors with the help of ^{31}P and ^{1}H MRS. Moreover, some metabolic ratios may be more specific markers for differentiation grade or metastatic capacity alone. Although it is difficult to extrapolate animal data to the human situation, these in vitro findings may give a lead for the in vivo studies on human prostate cancers.

Chapter 4

IN VITRO PROTON MAGNETIC RESONANCE SPECTROSCOPY OF FOUR HUMAN PROSTATE CANCER CELL LINES

INTRODUCTION

The recent development and clinical introduction of transrectal probes not only improved the quality of magnetic resonance imaging (MRI) of the human prostate but also made this organ accessible to magnetic resonance spectroscopy (MRS) [105 107 147 148] Transrectal MRI and MRS, basically employing the same instrumental set-up, are potential powerful non-invasive methods for monitoring the diseased prostate First to identify with MRI the suspected lesion and secondly to monitor with MRS the metabolism of this lesion Changes in various metabolic pathways associated with several cancers have been reported [110 141 142] For prostate cancer, metabolic derangements might provide markers that improve diagnosis and allow more accurate prediction of its clinical behaviour In vitro and in vivo studies employing ^{31}P, ^{1}H and ^{13}C MRS have shown that differences in the metabolic content of human prostate tissue samples correlated with tumor grade [75 46 82 105 107 145 146 153 154] Moreover, for the Dunning R 3327 rat tumor model it has been demonstrated that the relative levels of phosphocreatine, glycerophosphorylglycerol, glycerophosphoethanolamine and glycerophosphocholine, obtained by ^{1}H and ^{31}P MRS, can be used to differentiate sublines by differentiation grade, androgen sensitivity and metastatic capacity [77 161] However, interpretations of differences in MRS spectra between human prostate tissues with different biological behaviour are hampered by tissue heterogeneity and the lack of a complete understanding of the biochemical pathways MRS examinations of well defined human model systems are therefore needed to allow correlations between metabolic patterns and biological behaviour For this reason, studies of human prostate (cancer) cell strains are of value Yacoe et al investigated cell strains derived from human prostates to investigate whether ^{1}H MRS could reliably distinguish normal prostate epithelium from prostate cancer [174] In the present study we attempted to identify differences in metabolites which correlated with different biological behaviour, e g androgen responsiveness and morphology, in *human* prostate cancer Four well established human prostate cancer cell lines were characterized with in vitro proton MRS and metabolic differences were correlated with their biological behaviour

Materials and Methods

Tumor Cell Lines

Four established human prostatic carcinoma cell lines, PC-3, DU 145, TSU-Pr1 and LNCaP were used in this study [66 69 77 104] The characteristics of the four cell lines are summarized in table 1 Cells were maintained in RPMI 1640 culture medium supplemented with 10% foetal calf serum, 2 mM L-glutamine, 100 IU/ml penicillin, 100 μg/ml streptomycin and 250 nM dexamethasone at 37°C in 6% CO_2 at 99% relative humidity

Table 1. Characteristics of the four human prostate cancer cell lines used

Cell line	Origin	Histology of orig tumor	Doubling time (hours)	Androgen respons	PSA producing
LNCaP[66]	Lymphnode	moderate	50 1 ± 8 0	+	+
DU-145[164]	Brain	poorly	28 7 ± 2 9	−	−
PC-3[72]	Bone	poorly	35 2 ± 6.7	−	−
TSU-PR1[69]	Lymphnode	poorly	26 4 ± 4 5	−	±

Preparation of tissue extracts

After reaching a confluency of 70-80%, cells were harvested for perchloric acid (PCA) extraction as described previously [25] In short, single cell suspensions were obtained by trypsinization (0 25% trypsin/0 1% EDTA) and immediately washed three times with ice cold 0 9% NaCl to remove all the medium components The total number of cells varied between 4 6 x 10^6 cells Viability, as determined by the trypan blue dye exclusion test, was always ≥ 95% After centrifugation of the single cell suspension, the cell pellet was frozen in liquid nitrogen and stored at -80°C until time of extraction

The cell pellet was transferred into an all glass homogenizer and 4 ml ice cold 0 25 M PCA was added dropwise Cell homogenization was achieved at -80°C in approximately 30 minutes After centrifugation (12,000 g, 15 min, 4° C) of the cell extract, the pellet was discarded and the pH of the supernatant was immediately adjusted to 7 5 with 2 5 M KOH The PCA precipitate was centrifuged (12,000 g, 15 min, 4° C) and the supernatant was passed through a Chelex sample preparation disc (Bio-Rad Laboraties, Richmond, USA) and lyophilized Lyophilizates were dissolved in 500 µl 40 mM potassiumphosphate pH 7 0 The pH was corrected to pH 6 90-7 10 if necessary by addition of HCl or KOH The samples were lyophilizated again and stored at - 20° C

3 ml samples of culture media of all prostate cancer cell lines investigated was lyophilizated and stored at 20° C

Just before the ^{1}H MRS measurements, the lyophilizate was carefully thawed and dissolved in 500 µl D_2O containing 1 6 mM 3-(Trimethylsilyl) propionic acid-d4 sodium salt (TSP)

^{1}H NMR measurements

^{1}H NMR spectra were acquired on a 500 MHz spectrometer (Bruker AM500) and were recorded with a standard 5 mm ^{1}H NMR probe The spectra were recorded employing a 45° flip angle (6 µs) and a 7 28 sec pulse repetition time The resonance of H_2O was suppressed by low power continuous wave presaturation For the spectrum of each PCA extracted cell sample 900 scans were accumulated The chemical shifts

were referenced with respect to the chemical shift position of the TSP resonance.
^{1}H NMR spectra were further evaluated employing the NMR1 package (New Methods Research, INC, Last Syracuse, NY, USA) on a SUN Sparc station 330 (Sun Microsystems, INC, Mountain View, USA). Free induction decays (FIDs) were Fourier transformed after zero-filling from 16 K to 32 K and the application of a Lorentzian to Gaussian transformation filter. The spectra were semi-automatically fitted to Gaussian lineshape model functions Relative resonance integrals of proton metabolites of interest are expressed as ratios to the integral resonance of TSP.

Statistical analyses

Differences in ratios of metabolites between the different cell lines were investigated by the Wilcoxons rank test. Due to multiple testing $P < 0.01$ was considered as statistically significant.

RESULTS

PCA extracted cell lines

MR spectra of PCA extracts of four human prostate cancer cell lines were recorded and for each cell line at least five different passages were investigated. A 500 MHz proton MR spectrum of a PCA extract of the LNCaP cell line, with two expanded parts, is shown in figure 1. Resonances of some main metabolites could be identified with data from the literature.[25,40]
For each compound the best resolved resonance(s) were selected for quantitation purposes. Table 2 lists relative peak area integral ratios involving the doublet of the CH3 group of **lactate** (Lac) at 1.33 ppm, doublet of the CH3 group of **alanine** (Ala) at 1.49 ppm, quartet of the CH2 group of **citrate** (Cit) at 2.54 ppm, singlet of the CH3 group of **(phospho)creatine** at 3 04/3 05 ppm), singlets of the CH3 group of **phosphocholine** (PC) and **choline** (Chol) at 3.23 and 3 22 ppm respectively, triplet of Several differences were found between MRS spectra of the PCA extracted human cell lines. This is illustrated in figure 2 where ^{1}H MRS spectra of one LNCaP (A) and one TSU PCA extract (B) are shown.

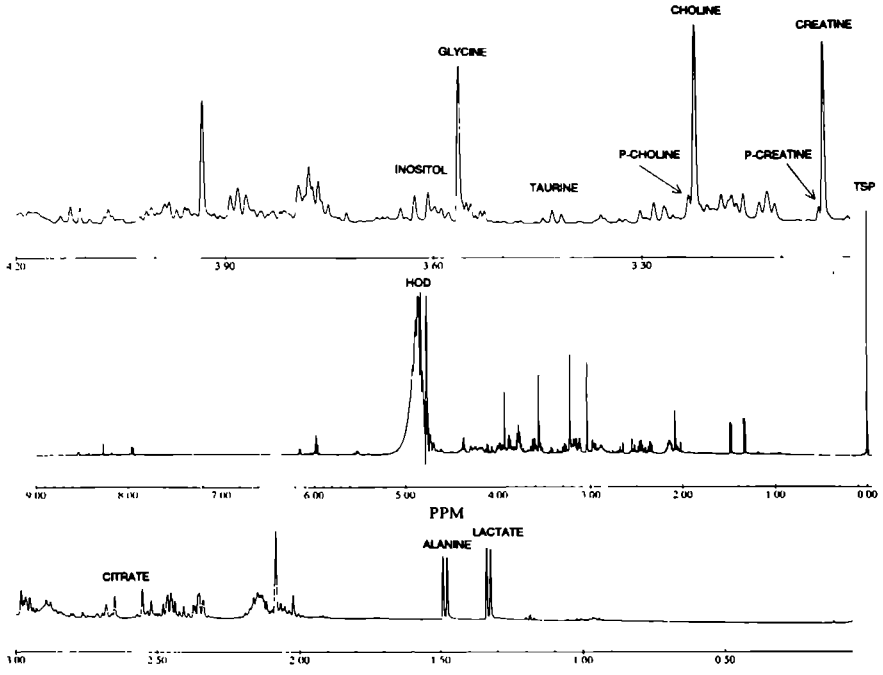

Figure 1: In vitro ^{1}H MR spectrum with peak assignments of PCA extract of LNCaP human prostate cancer cell line.

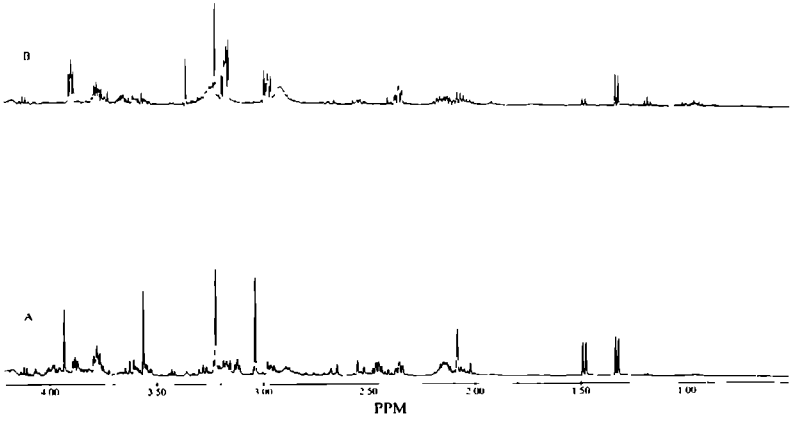

Figure 2. In vitro ^{1}H MR spectra of PCA extracts of LNCaP cell line (A) and TSU cell line (B).

The first prominent observation was the relative high amount of total creatine (TCr = PCr plus Cr) in the PCA extracts of LNCaP cells (table 2) The TCr / TPS ratio appeared to be significantly higher for the LNCaP cells samples when compared with the other three cell lines ($p < 0.01$)

Secondly, citrate resonances were absent in the MR spectra of PCA extracts of the PC-3, DU-145 and TSU cell lines, whereas only in one of the five samples of the LNCaP cell line citrate could be detected in the MR spectra Since citrate can rapidly diffuse from the prostate cell into the culture media also all media were spectroscopically examined ^{1}H MR spectra of the culture media of the LNCaP cells showed citrate resonances whereas in all the media of the other three cell lines no citrate resonances were detected (results not shown)

Finally, several differences in metabolic content of PCA extracts of DU-145, TSU and PC-3 cells were found The relative amount of taurine was significantly higher for the DU-145 PCA cell extracts when compared with the PC-3 and TSU (all $p < 0.01$) PC 3 and TSU cell extracts differed significantly from each other for inositol and creatine content, whereas the creatine content of DU-145 PCA extracts was also different from TSU PCA extracts ($p < 0.01$, table 2)

Table 2. Mean of metabolite ratios (range between brackets) of four human prostate cancer cell lines

	LNCaP		DU-145		TSU-PR1		PC-3	
lac/tsp	94	(18-169)	34	(11-67)	25	(14-46)	12	(6-56)
Ala/tsp	84	(18-164)	11	(7-23)	6	(4-19)	5	(1-9)
Citr/tsp	0	(0-72)	0		0		0	
Cr/tsp	60	(36-132)	9	(2-11)	0		10	(3-37)
Chol/tsp	40	(18-69)	12	(9-23)	22	(15-26)	16	(7-56)
PChol/tsp	6	(3-9)	5	(4-9)	4	(0-7)	3	(1-10)
Ino/tsp	0	(0-140)	156	(6-406)	0	(0-20)	44	(21-53)
Tau/tsp	11	(0-43)	84	(20-224)	0	(0-5)	0	(0-13)
Gly/tsp	48	(0-107)	7	(0-13)	5	(0-9)	6	(3-10)

DISCUSSION

Prostate tumors present sharp interindividual variations in biological behaviour and response to therapy At least 20-25% of the patients where hormonal treatment is the first choice therapy will not react and an equal percentage becomes resistant to the

treatment within 2 years [19 135] Therefore, new diagnostic methods able to predict more accurately the biological behaviour of the tumor are needed since these may lead to a better basis for individual treatment

We examined four well characterized human prostate cancer cell lines with ^{1}H MRS An in vitro approach was chosen because ^{1}H MRS of biological material may produce complex spectra, which are difficult to resolve in vivo Assignments for the same main metabolites were made as found earlier for human prostate cancer [75]

In this panel of PCA extracted human prostate cancer cell lines the relative level of total creatine was found to be discriminative for hormone sensitivity Vigneron et al found by in vivo ^{31}P MRS, an increased PCr / ATP ratio in one hormone sensitive Dunning tumor subline when compared to one hormone insensitive subline [169] Androgen deprivation (orchiectomy) resulted in a significant decrease of this ratio [169] However, in a recent in vitro MRS study, where three different hormone sensitive and four different hormone insensitive Dunning sublines were investigated no specific correlation for hormonal sensitivity with relative metabolite levels, including the PCr / ATP ratio, could be made [27] A correlation of increased PCr concentration and hormone sensitivity has also been suggested for rat breast cancer [137] Creatine levels can presently be detected in ^{1}H MR spectra recorded with transrectal probes, hence in vivo human MRS studies can now test the relevance of these in vitro observations [62]

Previous biochemical and MRS studies have suggested that the metabolism of citrate may be altered in prostate cancer [23 25 29 49 82 93 145] Citrate is a secretory product of the prostate and its production and secretion are under androgenic control [29] Testosterone stimulates the net citrate production and might also play an role in the citrate secretion [29] Normally citrate is present in human prostate tissue in high concentrations [23 29 49] In culture however, citrate can rapidly diffuse from the prostate cell in the culture media [49] It is therefore obligatory to measure both citrate levels in prostate (cancers) cells and in their culture media in studies with cultured prostate (cancer) cells In the present study, citrate resonances were absent in the MR spectra of PCA extracts of DU 145, PC-3 and TSU cells and in their culture media Kurhanewicz et al already showed that citrate signals could not be observed in ^{1}H MR spectra of DU 145 xenografts, either in vivo or in PCA extracts [82] In contrast, in one of the five LNCaP extracts a MRS detectable level of citrate was found and all the media of LNCaP cells showed citrate resonances in the MR spectra, suggesting that the hormone dependent LNCaP cells have a higher relative level of citrate compared to the other three hormone insensitive cell lines Early studies already suggested that citrate is reduced in early prostate cancer and nearly absent in advanced disease, which are known to have only a small portion of hormone sensitive cells [23 29 93] Possibly there is a difference in citrate content between hormone responsive and non-responsive prostate cancers Our present finding seem to fit well with this hypothesis and the aforementioned studies However, further in vivo MRS studies should be performed to compare the citrate concentrations in tumors of patients which are

escaped from hormonal treatment versus patients which do respond well to validate this finding

Finally, each prostate cancer cell line has its own metabolic fingerprint, e g several differences in metabolic content were found irrespective their biological behaviour The most striking difference was the high taurine content of the DU-145 cell extracts compared to both the PC-3 and the TSU cell extracts Kurhanewicz et al also showed large taurine resonances in the in vivo and in vitro ^{1}H MRS spectra of DU-145 tumor The difference in taurine content might be explained by differences in origin of the metastasis [66 69 72 164]

In conclusion, this MRS study of PCA extracts of four human prostate cancer cell lines demonstrate that, although each cell line has it's own metabolic fingerprint, the **creatine / tsp and citrate / tsp** ratios can be used to discriminate the androgen dependent LNCaP cell line from the other androgen independent cell lines Clinical MRS studies with transrectal probes now have to be performed to determine whether it is possible to discriminate cancers which will respond to androgen therapy based on their relative citrate and creatine content

Chapter 5

EFFECTS OF HIGH ENERGY SHOCK WAVES ON TUMOR BLOOD FLOW AND METABOLISM; $^{31}P/^{1}H/^{2}H$ NUCLEAR MAGNETIC RESONANCE SPECTROSCOPY STUDY.

INTRODUCTION

High energy shock waves (HESW) are of interest in the development of new experimental tumor treatment modalities Generated extracorporally and focused on a well-defined limited volume in the body, HESW can be used to influence tumor growth and response to therapy in vivo [34 37 67 130 142] Studies using tumor models in animals have shown that, at a constant acoustic energy output, HESW have a dose dependent tumor growth suppressive effect, whereas treatment with a higher number of HESW or with the same number at different time intervals results in a more prolonged tumor growth inhibition [121 169] In addition, combination with chemo- or cytokine-therapy resulted in more pronounced and even synergistic anti-tumor effects [120 122]

As nuclear magnetic resonance spectroscopy (NMR) enables to monitor changes in tumor metabolism in a longitudinal way it is a suitable technique for the evaluation of tumor therapies [56] Recently, using in vivo ^{31}P NMR, we have shown that the administration of HESW, focused on the centre of NU-1 human kidney cancer xenografts resulted in a significant, dose dependent, temporary reduction in high-energy phosphates, concomitant with an increase in inorganic phosphate (Pi) levels and a decrease in intra-cellular pH These changes occurred immediately after HESW exposure and preceded the suppression of tumor growth [155] These metabolic changes are qualitatively similar to those produced by ischemic inhibition of energy metabolism and suggest functional vascular changes following HESW exposure Histological examinations in various tumor models clearly reveal structural abnormalities at a vascular level after HESW treatment and suggest that vascular damage in the tumor may be the primary cause in promoting tumor necrosis [34 67 121] Thus, it is likely that the effects of HESW at the vascular level impair tumor cell metabolism

In this study we tried to confirm the hypothesis that an important target of HESW involves the functionality of the vascular component of tumors Tumor blood flow (TBF) and perfusion can be measured directly by ^{2}H NMR monitoring of D_2O applied to the tumor [43 76 77]

We have used this method to investigate the extent and duration of the effect of HESW on TBF After intra-tumoral injection of D_2O as a freely diffusible tracer, the clearance of $^{2}HO^{1}H$ was monitored By using mathematical (multi-)compartment models, this technique has shown to be a sensitive and reproducible method in the determination of TBF and perfusion [42 76 77]

As a direct metabolic consequence of the reduced TBF and oxygenation an increase in anaerobic metabolism and lactate production is expected Therefore, we also estimated the tumor lactate concentrations by ^{1}H NMR before and after HESW treatment In addition, the ^{1}H NMR measurements were combined with ^{31}P NMR measurements in

order to investigate the relation between lactate levels and pH as a function of time

MATERIALS AND METHODS

Animals

Xenografts were transplanted in six to eight week old male BALB/c athymic mice (Bornholtgårt, Ry, Denmark) The mice were kept in groups of five in PAG type 2 cages covered with an iso cap (Ifta Credo, France) for sterile conditions The mice were fed ad libitum with irradiated SRM-A MM food (Hope Farms, Woerden, The Netherlands) and drinking water was acidified (pH 3)

Tumors

The human renal cell carcinoma NU-1 xenograft was established in our laboratory by subcutaneous implantation of small tumor pieces derived from a tumor nephrectomy specimen Histologically the tumor is characterized as sarcomatous [120] For the HESW studies, tumors were implanted subcutaneously as trocar pieces at the upper part of the hind limb Passages 40-48 in vivo were used The three dimensions of the tumor were determined with a precision sliding calliper by measuring the maximum diameter and the diameters perpendicular to it The tumor volume was calculated by the equation (LxWxH) x (π/6) As in our earlier NMR experiments, tumors were allowed to grow to a volume of 250-300 mm^3 (mean 275 mm^3)

HESW treatment

The studies presented here were performed on a shock wave generator specially designed for experimental animal and in vitro studies The principles of the experimental set-up, the way of administration of the shock waves, and the positioning of the tumors in the focal area were described earlier in detail [121]

In contrast to those experiments, we now used an electromagnetic HESW generator modified from the clinical available Lithostar *plus* (Siemens) With this experimental generator higher pressure amplitudes can be obtained in a smaller focal area The physical principles and the definition of the parameters of its acoustic field were described elsewhere [124 166] Standardization and control of the acoustic field was assured by pressure measurements performed before each experiment Although the focus (defined by isobar lines representing 50% of the P_{max}) is somewhat smaller, the total acoustic energy is equivalent to that of the Lithostar and, assuming that the pressure profile and energy are the main determining factors, we compared the outcome of the experiments with our previous results Tumors were treated with 800 HESW focused centrally on the tumor (treatment) Sham treatment was achieved by placing the tumor in such a way that the focus (as determined by pressure measurements) did not

encounter the tumor. Just before HESW (sham-)exposure, mice were anaesthetized with ketamine hydrochloride (Ketalar, Parke-Davis) 100 mg/kg for a 15 minute period.

NMR Spectroscopy

In vivo NMR spectroscopy was performed on a 4.7 tesla Bruker WM-200 spectrometer as described previously.[155] The mice were anaesthetized by means of a gas flow of 1.5% enflurane in a O_2/N_2O mixture applied through a nosecone. Body temperature was monitored by a rectal probe and kept at 36-37°C by a flow of humidified warm air. The tumors were exposed through a matched hole in a Faraday shield and positioned partly inside the radio-frequency (RF) coil to prevent any contribution of signals from surrounding tissue. The magnetic field homogeneity was optimized by using the ^1H NMR signal from tumor H_2O. Typical linewidths of this signal were 0.1 - 0.2 ppm. The animals were spectroscopically examined before and 4 to 6 times after administration of HESW.

^2H NMR.

The deuterium measurements were performed at a resonance frequency of 31 MHz, employing a home-built probe with a 1H / 2H double tunable three-turn solenoidal coil with an inner diameter of 13 mm. After optimizing the field homogeneity the RF probe was removed from the magnet and the tumors were injected outside the magnet with 10-20 μl isotonic saline $^2HO^1O$ solution at a single site (tumor centre) or at three sites (concentric) using a micro-syringe. During this procedure the tumors remained in their original position in the RF coil. The probe was repositioned in the magnet and serial ^2H NMR measurements were started 90 seconds after injection.

Deuterium spectra were collected in 45 second time blocks with 64 scans/block using a 10 μs RF pulse, 2K data points and a spectral width of 5000 Hz.

$^1H/^{31}P$ NMR.

Lactate detection by ^1H NMR and pH measurement by ^{31}P NMR were performed at 200 and 80 MHz respectively, employing a home-built ^1H / ^{31}P double tunable two-turn surface coil with an inner diameter of 10 mm.

The ^1H methyl signal of lactic acid has to be resolved from the co-resonating methyl signals of triglycerides from subcutaneous adipose tissue. For spectral editing of the methyl signal of lactate the spin-echo difference spectroscopy method was used.[63] The spin-echo RF pulse sequence was preceded by a CHESS sequence to reduce the H_2O signal[59] and RF pre-pulses to reduce high flux signals.[8,148] The prepulses and excitation pulse were all hard pulses.[12] Further H_2O suppression was provided by the use of a 1-1 refocussing pulse. Selective inversion of the methine (α) protons for lactate editing was achieved with a rotating-phase DANTE.[10] In this way, on and off resonance inversion is realized by clock- and counter-clockwise phase rotation. During the

experiment the RF carrier frequency was set at 3.75 ppm upfield from the water signal. The spin-echo time was 152 msec and the scan repetition time was 2.5 seconds. This way of lactate editing was found to be highly effective in the selection of the CH_3 signal of lactate from the dominating methylene proton signals of triglycerides. In all cases the reliability of the sequence to detect the lactate methyl protons was tested by shifting the DANTE excitation band away from the 4.1 ppm position of the α lactate proton.

In order to estimate the absolute concentration of lactate, a ^1H NMR spectrum without H_2O suppression was also recorded with the same spin-echo sequence to obtain the tissue H_2O resonance. To avoid interference of H_2O spin relaxation with the quantification of lactate a short echotime (1 msec) and a long scan repetition time (7 seconds) were chosen.

Measurements of the T_2 relaxation time of tumor water proton spins were performed with a CPMG pulse sequence. The time delay time between the 180° pulses was set to 2 ms. Data was acquired for 8 echo times between 8 and 320 ms.

^{31}P NMR spectra were obtained as previously described[155] with a composite 90° pulse with a nominal 90° pulse at about 1 mm from the coil centre. The pulse repetition time was 3.5 seconds and the spectral width was 5000 Hz acquired with 4K data points. Typically 256 or 512 scans were acquired.

DATA ANALYSIS

Most NMR data was analyzed on an Aspect 3000 computer using standard Bruker software. For ^{31}P NMR convolution difference was applied to remove broad spectral components using a line broadening of 300 Hz. In order to improve the signal-to-noise ratio, an exponential multiplication was used resulting in a linebroadening between 20 and 30 Hz

For ^1H NMR an exponential multiplication was applied resulting in a linebroadening between 1 and 2 Hz. Water T_2 relaxation times were obtained by fitting the integrals of the H_2O signals, obtained by the CPMG sequence, to a monoexponential decay function.

Of the data obtained in the deuterium wash-out experiments, every first and each following fifth deuterium spectrum recorded, were evaluated employing the NMR1 package (New Methods Research, INC, Last Syracuse, NY, USA) on a Sun Sparc station 330 (Sun Microsystems, INC, Mountain View, USA). FIDs were Fourier transformed and the phase was manually corrected. Deuterium resonances were semi-automatically fitted to Lorentzian lineshape model functions. Integrals of the deuterium resonance were calculated and plotted as a function of time.

DOH wash-out and TBF

Tumor blood flow was determined using compartment kinetic models taking tracer recirculation into account as described by Kim and Ackerman [76,77] In all cases the tumor deuterium residue wash-out could accurately be described by

$Q(t) = a\,e^{\alpha t} + b\,e^{\beta t}$ (and $\alpha > \beta > 0$)

This equation describes a flow model which represents (non-communicating) fast and slow flow compartments in the tumor, where Q(t) is the quantified deuterium residue at time t, and the half-life times of the tracer in the fast and slow flow compartment are $Tf = {}^{\ln 2}/_{\alpha}$ and $Ts = {}^{\ln 2}/_{\beta}$ respectively

The (volume) fractions of the fast and slow components can be expressed as ${}^{a}/_{a+b}$ and ${}^{b}/_{a+b}$

The initial half life (t = 0) is defined by ${}^{\ln 2}/_{\tau}$ where τ is the weighed average $({}^{a\alpha + b\beta}/_{a+b})$ of α and ß

The formula TBF = 100 x lambda x τ is then an estimate of the initial tumor blood flow (in units of ${}^{ml}/_{100g \times min}$) Here lambda is the tumor-to-blood partition coefficient (ratio of the water weight of a unit mass of tumor to the water weight of a volume of blood) which was determined by measuring wet and dry weights of tumor and blood Dry weights were achieved by drying in an oven at a temperature of 90°C Lambda was calculated to be 0 906 ± 0 019 (in units of ${}^{ml}/_{g}$ (n=5) Per animal, the half lifes were calculated using (nonlinear) least squares regression

Tumor lactate quantification

In order to estimate the absolute lactate concentration in the tumor, the resonance intensity of the lactate signal was related to the intensity of the water resonance

The lactate concentration, expressed per tumor volume, was calculated by the following formula $[lactate] = IF \times e^{-t_e/T2lact} \times F_c \times {}^{2}/_{3} \times \{RV_t/RV_w\} \times [H_2O]$

T_{2lact} is the spin-spin relaxation time of the methyl proton spins of lactate, t_e is the echo time The lactate signal is recorded with a spin echo sequence having a t_e of 152 msec and hence T_2 weighted Corrections can be made if the T_2 value is known Adequate T_2 relaxation time measurements of the methyl signal of lactate in subcutaneous tumors requires suppression of J modulation in conjunction with editing from triglyceride signals Presently we have not yet implemented this addition and have adopted a T_2 value of 150 msec which is close to T_2 values as determined for the methyl signal of lactate in the rat brain at 4 7 T [171]

The inversion factor (IF) was set at 0 8 In control experiments with lactate solutions we observed that complete inversion of the methyl resonance of lactate by the application of the DANTE sequence could not be achieved About 80% of the original lactate signal intensity was recovered after editing This result is similar to experiments of Hanstock et al [61] who also used a DANTE sequence for inversion with a surface coil

F_c is the excitation profile correction due to the 1-1 pulse which is necessary because

the RF carrier was not exactly at the resonance position of the methyl protons of lactate The factor $/_3$ corrects for the fact that water has 2 protons and the lactate methyl group 3 RV_l and RV_w are the resonance integral values of the methyl group of lactate and water respectively $[H_2O]$ is the concentration of water per tumor volume Tumor lactate was also measured employing ^1H NMR, after perchloric acid extraction (PCA) of freeze clamped tumor xenografts [11] Before extraction tumors were weighted and a calibration standard (2 mM 3 (Trimethylsilyl) propionic acid-d4 sodium salt) was added to the extract solution

Phosphate energy metabolism and pH.

The assignments of the resonances and the calculation of the tissue pH from the inorganic phosphate (Pi) signal chemical shift in the ^{31}P NMR spectra were performed as described before [155]

Statistics

Due to the nonnormality of the statistical distribution, Wilcoxon s test was used to compare the DOH wash out parameters in both groups For the same reason the lactate concentration and pH data were analyzed using the Koziol test

Statistical significance was set at $p < 0\ 05$

RESULTS

Effects of HESW on TBF

To determine the reproducibility of the DOH wash-out method after intra tumoral injection of the tracer, D_2O was injected into the tumor at subsequent time intervals (3 hours) We observed no difference in DOH wash out curves (data not shown) The DOH profiles were best fitted using the expression describing two components in the wash-out In this model a fast flow and slow flow component are characterized by their half life times (expressed as Tf and Ts of the tracer) and their (volume) fraction In each individual tumor a similar wash out was found either using single or multiple site injections In the following experiments DOH was injected at three sites in the tumor

Figure 1 shows representative data of two individual tumors, obtained before and after treatment with 800 HESW focused adjacent to the tumor (sham) or central on the tumor (treated) No significant differences in DOH decay before and after sham treatment were detected (figure 1a) In contrast, after the application of 800 HESW at the centre of the tumor, a significant decrease in wash out was observed during the first 24 hours after treatment After 48 hours the wash-out curves showed pretreatment values (figure 1b)

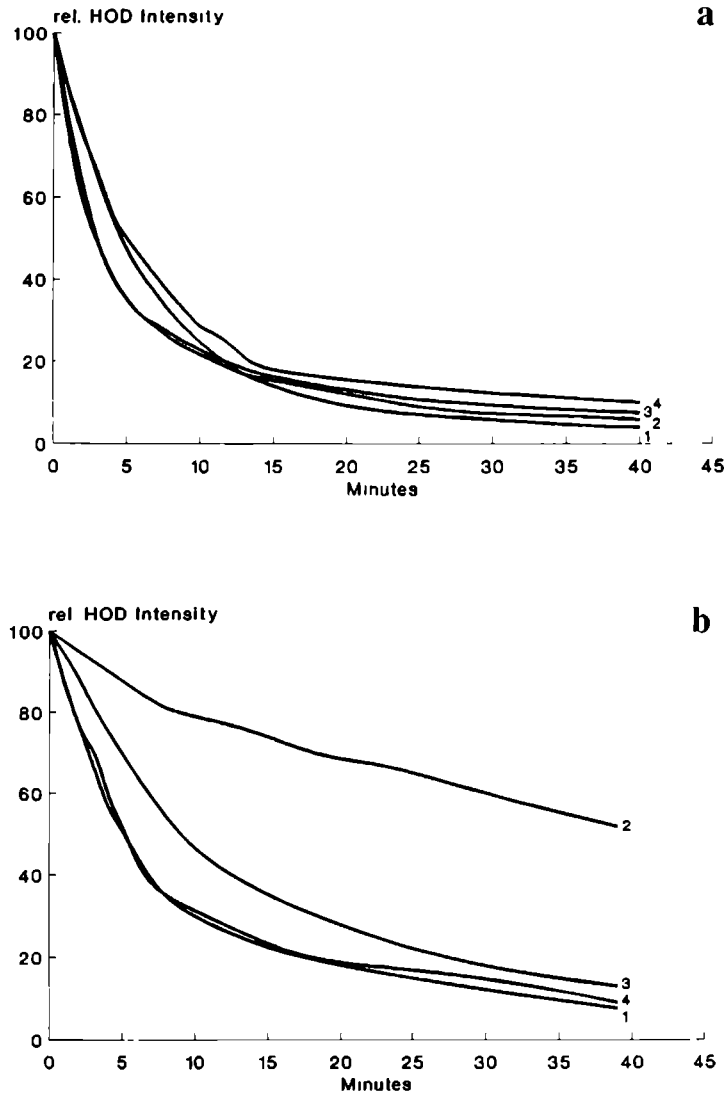

Figure 1. Representative figures of relative HOD intensity in time detected by ^2H NMR spectroscopy after intra-tumoral injection of an isotonic D_2O solution before (1), as well as at two (2), twenty-four (3), and forty-eight (4) hours after HESW exposure adjacent to the tumor (fig 1a, sham-treatment) or central on the tumor (fig 1b, treated)

Figure 2 shows the mean calculated tumor blood flow (ml/100g.min) before and after exposure (n=5 for each group) The mean pretreatment TBF value of the sham and of the treated group were slightly different but this was not significant (Wilcoxon; p=0 89).

Treatment with 800 HESW adjacent to the tumor resulted in an increase in mean TBF. However, these changes were not significant. After shock wave exposure to the centre of the tumor, the mean TBF decreased with approximately 75% after 2 hours and afterwards increased to 50% after 24 hours as compared to the mean pretreatment TBF As a result, TBF levels in the treatment group were significant lower than in the control group (Wilcoxon; $p<0.005$ and $p<0.05$ respectively).

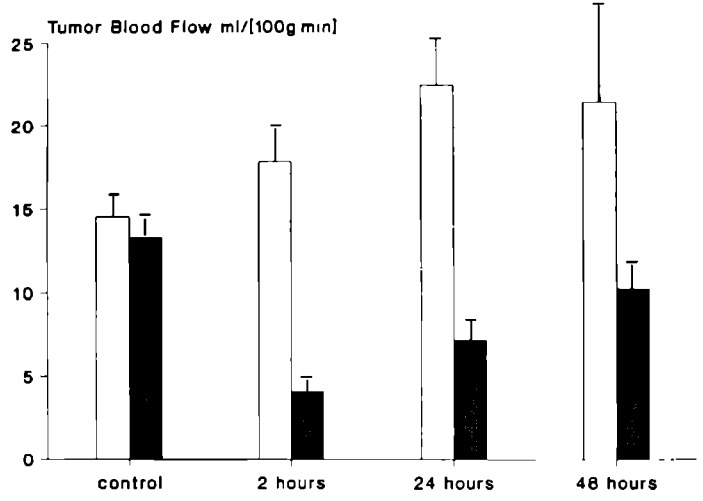

Figure 2. NU-1 kidney cancer xenograft tumor blood flow (in units of $^{ml}/_{100g\,x\,min}$) before (control) and after treatment with 800 HESW (white bars· sham-treated group, black bars· treated group) D_2O was injected at three sites intra-tumoral and TBF was calculated from the fitted bi-exponential wash-out curves Values are mean ± standard error of the mean (each group n=5)

In order to detect a possible differential impact on the fast and slow component of the DOH wash-out we evaluated the bi-exponential wash-out in more detail. In Table 2 the half life times of the tracer in the fast and slow compartment (Tf respectively Ts) as well as the volume fraction of the fast component before and two hours after treatment are presented. Two hours after exposure to 800 HESW a significant higher Ts and smaller volume fraction of the fast flow component (Wilcoxon; p=0.01 and 0.02 respectively) were seen. The remaining fast fraction showed no significant

differences in Tf Similar analysis of these parameters for the subsequent period (10 hours or more) revealed no clear patterns

Table 1: Median half life times of the tracer (DOH) in the fast and slow compartment (Tf resp Ts) as well as the volume fraction of the fast component before and two hours after treatment

		PRE-TREATMENT			+2 HRS		
		Tf	Ts	fraction	Tf	Ts	fraction
Sham	(n=5)	4 1	45	86	3 9	21	80
Treated	(n=5)	3 4	33	74	2 7	52	09

The observations on TBF are in agreement with histology that has shown vascular disruption, stasis within capillaries and thrombosis immediately after HESW exposure [155] As these processes might affect relaxation times of water proton spins we studied T_2 relaxations times of water proton spins in the tumor in the hours after HESW (see table 2) A significant decrease is observed for this relaxation time thus providing an additional marker for early HESW effects

Table 2: Average T_2 relaxation times values in seconds (mean ± SD) of H_2O protons for three different NU-1 xenografts before and after exposure to 800 HESW

	before HESW	2 hrs after HESW	5 hrs after HESW
T_2 value	0 63 ± 0 03	0 59 ± 0 06	0 48 ± 0 09 $p < 0\ 05$

Effects of HESW on tumor lactate levels and pH

In figure 3 we show the effectiveness of lactate editing by the implemented spin-echo difference method By using selective inversion by the DANTE pulse train placed at 4 1 ppm and at -2 1 ppm, the lactate signal is obtained at 1 3 ppm in the difference spectrum No lactate signal is obtained after shifting the selective inversion to 3 8 ppm, thus confirming that the signal at 1 3 ppm originates from lactate

Tumor lactate concentrations were estimated as described in materials and methods From 8 independent measurements an average lactate concentration of 7 1 ± 1 9 mM was obtained for the renal tumor xenografts (pH ≥ 7 0 measured by ^{31}P NMR, results not shown) This value is of the same order as the lactate concentration measured in other subcutaneous tumor models [44, 96] For two in vitro NMR measurements of PCA extracts of the renal tumor xenografts we estimated the lactate concentration to be 5 4 and 7 8 mM These observations indicate that our in vivo determinations of lactate

concentration provides a good approximation for the actual lactate concentration despite the necessary assumption made for the T_1 relaxation time of lactate methyl proton spins in the tumor

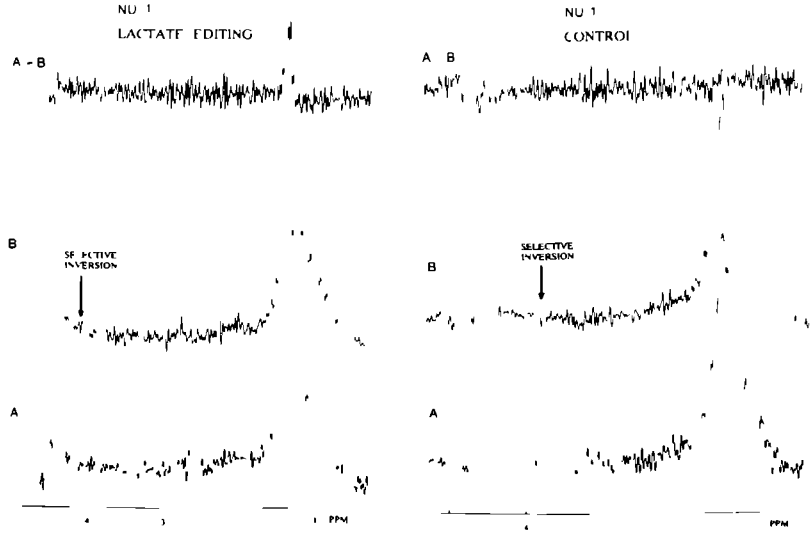

Figure 3. Editing in in vivo ^1H MR spectroscopy of NU 1 human renal cancer xenografts to resolve the methyl group resonance of lactate from resonances of triglycerides

Left Lactate editing experiment Selective inversion by the DANTE pulses placed at 4 1 ppm (B) to invert the methine spins of lactate and at -2 1 ppm (A) for off resonance inversion The lactate signal is obtained at 1 3 ppm in the difference spectrum (A-B)

Right Control experiment No signal is observed at 1 3 ppm in the difference spectrum (A-B) after shifting the selective inversion to 3 8 ppm thus confirming that the signal at 1 3 ppm obtained in the previous experiment originates from lactate

The effect of HESW treatment on lactate levels and tumor pH was determined simultaneously by combining ^{31}P and ^1H NMR (see fig 4A) There was no statistical significant difference for pH and lactate pretreatment levels between the sham treated and HESW treated group

HESW treatment resulted in a maximal increase in the average estimated lactate concentration from 8 8 mM (range 5 9 to 11 5) to 16 5 mM (range 14 9-17 9) 4 hours post treatment The lactate concentration decreased to pretreatment levels within the

following 48 hours In principle an increase of the lactate signal may be due to an increase in T_2 relaxation times of the methyl proton spins after HESW application but it would require substantial changes in T_2 to explain the intensity increases observed Note that the T_2 relaxation time of water proton spins does not increase after HESW exposure (see Table 2)

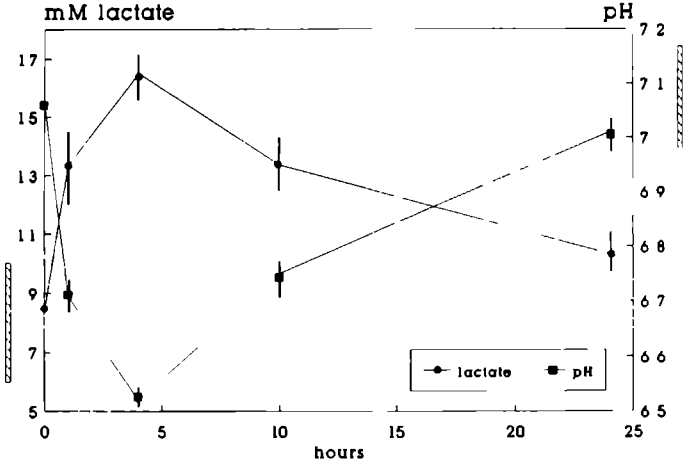

Figure 4A. Changes in lactate levels and pH, in the NU 1 kidney cancer xenograft after treatment with 800 HESW, focused on the centre of the tumor Values are mean ± standard error of the mean, (n=5) The dashed vertical bars represent the range of values after the sham-treatment procedure (n=5)

The changes in pH showed a similar, but inverse, temporal pattern as the increase in the estimated lactate concentration After 4 hours the mean pH was decreased from 7 06 (range 7 12 to 6 97) to 6 52 (range 6 45 to 6 60) Thereafter the pH increased to pretreatment values in a similar time span as the lactate concentration The Koziol test revealed a significant difference in the temporal pattern between treatment and sham-treatment for the lactate concentration as well as the pH (both $p < 0\ 001$). A plot of pH as a function of the estimated lactate concentration (Fig 4B) reveals a linear relationship between these two variables This suggests that pH changes are caused by variations in lactic acid content although HESW may generate protons from other sources, e g hydrolysis of nucleoside triphosphates, which may also contribute to pH changes Indeed the HESW induced temporary metabolic decline, as represented by the $^{NTP}/_{P_i}$ ratio, shows a similar time dependent pattern as lactate (data not shown, but see ref 155)

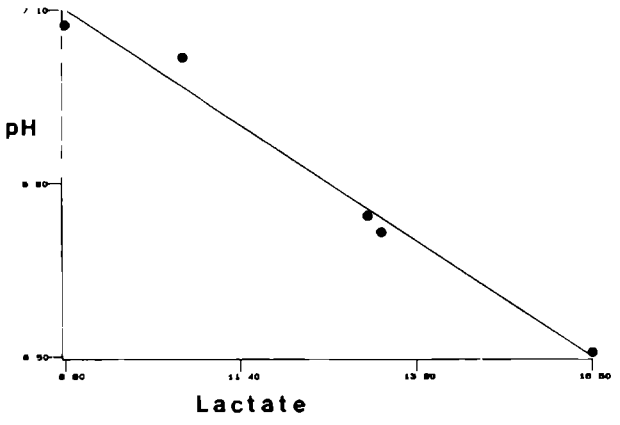

Figure 4B Plot of pH values and estimated lactate concentrations [mM] showing the linear relationship between these variables
The correlation coefficient for the linear correlation between lactate and pH is -0 9

DISCUSSION

Although HESW have been successfully used as an anti-tumor treatment modality in different animal tumor models, the mode of action of HESW is still largely unknown Recently, in vivo ^{31}P NMR spectroscopy in the NU-1 kidney xenograft showed drastic alterations in tumor cell metabolism, and a temporary tumor growth inhibition after HESW exposure [155] Since HESW, generated extra-corporally, can be precisely focused on a limited area in the body, these findings revealed a new potential application for this form of acoustic energy At present it is unclear whether the metabolic changes observed are a direct or an indirect effect of the shock waves The metabolic changes seem to be related to the induction of a temporary ischemia, due to an impaired tumor blood flow and perfusion

In the present study it is demonstrated that HESW causes a reduction in D_2O efflux from the tumor, a decrease in the T_2 relaxation time of tumor water proton spins and an increase in estimated lactate levels concomitant with a decrease in pH of the tumor tissue

D_2O efflux measurements by ^2H NMR can be used to evaluate TBF and perfusion in response to therapeutic interventions [42 68 118]

In our experiments, a bi-exponential tracer residue decay was observed after applying DOH intra-tumoral in non-treated NU-1 tumors The tracer wash-out was best described by a mathematical model using a fast and slow flow component of DOH decay within the tumor This wash-out pattern was not influenced significantly by the

number of D O injection sites Repeating the experiment after 5 hours also revealed similar DOH wash-outs Our results are in agreement with similar experiments in the RIF 1 tumor[77] and the bi exponential clearance kinetics are likely due to TBF heterogeneity [83]

The studies presented here show a pronounced effect of HESW on the TBF in the NU-1 human kidney cancer xenograft When the HESW were focused on the tumors, a mean reduction in TBF of 75% of the initial TBF two hours after HESW treatment was observed Exposure to 800 HESW focused adjacently to the tumor did not influence TBF significantly The reduction in TBF was temporary and the DOH wash-out increased to non treated profiles These results demonstrate that a reduction in TBF by HESW is only effectuated if the tumor (or at least a major part) is subjected to the high pressure focal area

In this study the major effect was seen in the fast flow component suggesting that the most viable part of the tumor with the highest TBF is most sensitive towards the shock waves

How can these effects of HESW on TBF be explained? Recent studies indicate that cavitation, presumably associated with the tensile pressure, have a damaging effect at the vascular level [38 177] In addition microscopic studies in the NU 1 xenograft as well as in several other animal tumor models have shown vascular (capillar) disruption extravasation of erythrocytes and the formation of thrombosis and necrosis when the tumors were placed in the focal beam with high pressures [34 67 170 171] Thus, the impact of HESW on functional vascularization (TBF) most likely results from the generation of cavitation which subsequently act on the tumor vascular component (damaging and or activation of endothelial cells) Whether more gas holding nuclei are present and thus cavitation are induced to a greater extent in the well perfused (fast compartment) parts of the tumor is speculative The ^{1}H NMR spectroscopy studies showed a temporary increase in lactate concentrations From this observation one can conclude that the reduction in TBF results in cellular hypoxia and that consequently anaerobic glycolysis becomes the main cellular energy source Since the TBF is reduced the increased lactate concentration could also be explained by a disturbed outflow of lactate However the concomitant monitoring of ^{31}P NMR revealed a synchronous temporary change in tissue pH (i e , *intra* cellular tumor pH), suggesting that an enhanced lactic acid synthesis is important in tissue acidification [65 96] The outcome of the $^{31}P/^{1}H$ NMR studies supports the hypothesis that the HESW induced tumor growth suppression is mediated by an impact on the functionality of the vascular component of the tumor

Quantitative measurement of TBF and perfusion may not only contribute to the knowledge of HESW induced changes in vascular functionality, moreover this may provide the rational for the use of HESW in a combined treatment setting, i e , combining HESW with chemo- or immunotherapy

Until now, as a result of the lack of knowledge on the mode of action, treatment schedules have been determined empirically The findings here presented can provide a better rational for developing more effective combined treatment modalities, e g , the use of HESW adjuvant to systemic drugs that have an increased effect in an acid environment, or that block glycolysis In addition to a diminished drug outflow, a decreased TBF and perfusion may also enhance diffusion processes and thus result in an enhanced drug penetration in the tumor

The extent of modulation of local TBF and perfusion provoked by HESW treatment, with subsequent changes in metabolism, will be of importance in designing adjuvant (local or systemic) anti cancer therapies

Chapter 6

THE EFFECTS OF SUCCESSIVE HIGH ENERGY SHOCK WAVE TUMOR ADMINISTRATION ON TUMOR BLOOD FLOW

INTRODUCTION

Experimental animal studies using different tumor model systems, have shown that temporal growth suppressive effects can be achieved by treating tumors with high energy shock waves (HESW) [34 37 67 121 143 171] Moreover combination of HESW with chemotherapy or cytokines resulted in additive or synergistic antitumor effects [4 85 120 123] A number of variables that influence these antitumor effects have been identified including tumor vascularization, time interval between successive treatments number of HESW, number of HESW foci tumor size and tumor model system [67 121 171]

Several studies have been performed to clarify the mode of action of HESW Gamarra et al demonstrated with the use of autoradiography of iodo [^{14}C] antipyrine a temporary reduction of the perfusion of A mel-3 tumors after treatment with HESW [53] Using magnetic resonance spectroscopy (MRS) techniques we found a temporary impairment of tumor blood flow (TBF) in the NU-1 renal cancer xenograft after HESW application, resulting in a metabolic inactivation and acidification of the tumor [155 157] Histological studies of this NU-1 tumor show changes in tumor vasculature due to HESW exposure i e disrupted capillaries, extravasation of erythrocytes distended microvessels with tightly packed erythrocytes and thrombi formation [170] Apparently, one of the main targets of HESW is the vascular system [34 53 67 121 144 155 157]

As mentioned above, earlier studies using different tumor models revealed that the antitumor effects of HESW could be enhanced by repeated HESW tumor treatments and that shortening of the interval between subsequent HESW treatments from 24 hours to 5 hours leads to more effective tumor growth inhibition [121 171] It is tempting to speculate that increased efficacy is associated with the extent and duration of the decrease of TBF after successive HESW exposures

We therefore evaluated the effects of repeated HESW application on TBF As in our previous MRS study, intra-tumoral injected deuterated water (D_2O) was used as a MRS detectable tracer for measurement of TBF [15] This technique has proved to be a sensitive and reproducible method in the determination of TBF and perfusion [44 78 83 108] Moreover since the MRS TBF measurement method is non destructive and relatively non invasive, it is possible to measure TBF in the same subject repeatedly It is therefore an ideal technique to monitor changes in tumor blood flow after repeated HESW tumor administrations

MATERIALS and METHODS

Animals

Xenografts were transplanted in six to eight week old male BALB/c athymic mice (Bomholtgårt, Ry Denmark) The mice were kept in groups of five in PAG type 2 cages covered with an iso cap (Ifta Credo, France) for sterile conditions The mice were fed ad libitum with irradiated SRM-A MM food (Hope Farms, Woerden, The Netherlands) and drinking water was acidified (pH 3)

Tumors

The human renal cell carcinoma NU-1 xenograft was established in our laboratory by subcutaneous implantation of small tumor pieces derived from a tumor nephrectomy specimen [70] For the HESW studies tumors were implanted subcutaneously as trocar pieces at the upper part of the hind limb Passages 9-14 in vivo were used The three dimensions of the tumor were determined with a precision sliding calliper by measuring the maximum diameter and the diameters perpendicular to it The tumor volume was calculated by the equation (LxWxH) x (π/6) Tumors were allowed to grow to a volume of 300-350 mm (mean 325 mm^3)

HESW

HESW were generated by an experimental set up of the commercially available electromagnetic shock wave source Lithostar *Plus* (Siemens AG, Erlangen, Germany) The physical and technical characteristics of this experimental shock wave source have been described recently [103] In short the main frequency of the pulse was 200 kHz (resonance frequency of the system) The focal area (defined as pressure 6 dB zone) was 4 x 40 mm (lateral x vertical) at maximum setting

Just before HESW (sham)exposure mice were anaesthetized with ketamine hydrochloride (Ketalar, Parke Davis) 100 mg/kg for a 15 minute period Mice were kept in fixed position in a plastic tube which was placed in the water bath The tumor bearing leg was projected through a hole in the basis of the plastic tube and the centre of the tumor was positioned in the focal area through a three dimensial positioning system Sham exposure was achieved by placing the tumor in such a way that the focus (as determined by pressure measurements) did not encounter the tumor Each HESW administration consisted of in total 800 pulses with an energy density of 0 47 mJ/mm^2 (pulse repetition frequency of 2 Hz) All experiments were carried out with degassed water at 37°C The NU 1 tumors were exposed twice to HESW (at T = 0 and T = 24 hours)

NMR Spectroscopy

In vivo NMR spectroscopy was performed on a 4 7 tesla Bruker WM-200 spectrometer as described previously [155] The mice were anaesthetized by means of a gas flow of 1 5% enflurane in a O_2/N_2O mixture applied through a nosecone Body temperature was monitored using a non-magnetic temperature probe and maintained at 37° C by a flow of humidified warm air The tumors were exposed through a matched hole in a Faraday shield and positioned partly inside the radio-frequency (RF) coil to prevent any contribution of signals from surrounding tissue The magnetic field homogeneity was optimized by using the ^1H NMR signal from tumor H_2O Typical linewidths of this signal were 0 1 - 0 2 ppm The animals were spectroscopically examined two hours before the first administration of HESW (T = -2) and at T=2, T=8, T=16, T=26, T=32 and T=40 hours

The deuterium measurements were performed at a resonance frequency of 31 MHz, employing a home-built probe with a 1H / 2H / 31P triple tunable three-turn solenoidal coil with an inner diameter of 14 mm After optimizing the field homogeneity the RF probe was removed from the magnet According to the results of Larcombe-Mc Douall and Evelhoch 60-70 μl PBS-D_2O was injected (concentric) intratumoral at three different sites, using a 30 gauss micro-syringe [83] During this procedure the tumors remained in their original position in the RF coil The probe was repositioned in the magnet and serial ^2H NMR measurements were started within 70 seconds after injection

Sixty-four deuterium spectra were collected in 49 second time blocks with 64 scans / block using a 10 μs RF pulse, 2K data points and a spectral width of 5000 Hz

Data Analysis

For each timepoint, every first and following fifth deuterium spectrum recorded, were evaluated employing the NMR1 package (New Methods Research, INC, Last Syracuse, NY, USA) on a Sun Sparc station 330 (Sun Microsystems, INC, Mountain View, USA) Free induction decays (FIDs) were Fourier transformed and the phase was manually corrected Deuterium resonances were semi-automatically fitted to Lorentzian lineshape model functions Absolute integrals of the deuterium resonance were calculated and plotted as a function of time The D_2O clearance curves thus obtained are presumed to represent blood flow within the whole tumor [83]

Clearance curves of D_2O were best fitted using a single compartment model Tumor blood flow was thus determined using a single compartment model as described by Kim and Ackerman [78] In all cases the deuterium residue wash-out could accurately be described by

$$Q(t) = Q_{bg} + [Q(0) - Q_{bg}] \times \exp(-kt)$$

This equation describes the simplest first order kinetic "single compartment model" where Q(t) is the tracer quantity at time t, Q_{bg} is the non zero steady-state tracer

background, Q(0) is that at t = 0 and k is the first order rate constant governing tracer wash out.[78]

Since the steady-state tracer background (residual from previous experiment) already have been subtracted from the original decay curve the deuterium wash out decay can be formulated as:

$Q(t) = Q(0) \times \exp(-kt)$

The formula TBF = 100 x lambda x k is then an estimate of the initial tumor blood flow (in units of $^{ml}/_{100gxmin}$). Here lambda is the tumor-to-blood partition coefficient (ratio of the water weight of a unit mass of tumor to the water weight of a volume of blood) which was determined by mea-suring wet and dry weights of tumor and blood. Dry weights were achieved by drying in an oven at a temperature of 90°C. Lambda was calculated to be 0.906 ± 0.019 (in units of $^{ml}/_{g}$ (n=5).

Statistics

Because of the normal distribution pattern of the calculated TBF, two-sided T test was used to compare the TBF between the control and HESW applicated group and to evaluate the effect of the second HESW administration. Statistical significance was set at $p < 0.05$.

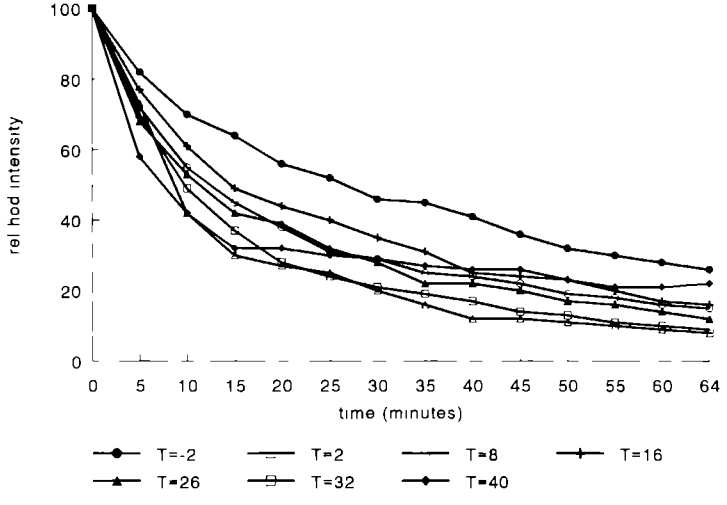

Figure 1. D_2O outflow curves, wit data points each 5 measurements, at 7 different time points of a ham treated control tumor obtained by ^2H MRS after intra-tumoral injection of an isotonic D_2O solution

RESULTS

According to the results of Larcombe-Mc Douall and Evelhoch 60-70 μl D_2O was injected intratumoral at three different sites, presuming that the D_2O clearance curves thus obtained represent blood flow within the whole tumor.[83] The D_2O clearance curves were best fitted using an one compartment model.

Tumor blood flow in control tumors

In Figure 1 seven D_2O outflow curves obtained at T= -2, T=2, T=8, T=16, T=26, T=32 and T=40 hours from one representative control NU-1 tumor are shown. Calculated mean TBF of all HESW non-exposed control tumors (N=5) for the subsequent time points revealed no significant changes in TBF during this time period (p=0.17, fig.2).

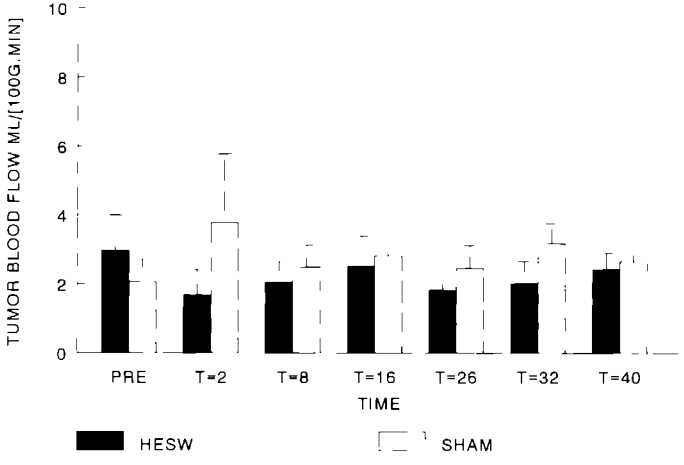

Figure 2. Calculated mean tumor blood flow (in units of ml/100gxmin) with SD of 5 sham treated control tumors (gray bars) and of five HESW treated tumors (black bars). Tumors were HESW or sham treated at T = 0 and at T = 24 hours.

Tumor blood flow in HESW exposed tumors

The mean pre (sham) HESW exposure TBF values in the HESW and control group were statistically not different (fig. 2). Administration of 800 HESW on the centre of the tumor resulted in a decrease of the mean TBF of 46 $\pm$ 19 % after 2 hours and 16 $\pm$ 30% after 16 hours. A second HESW exposure, 24 hours after the first, resulted in a decrease of the mean TBF with 37 $\pm$ 23 % after 2 hours and 16 $\pm$ 34% after 16 hours when compared to pre-exposure values. As a result, TBF levels two hours after the first and second HESW administration were significantly lower than the pre-

exposure TBF ($p=0.02$ and $p=0.04$ respectively). Moreover, comparing the effect on TBF of the first and second HESW administration revealed no significant difference ($p=0.45$).

DISCUSSION

Recently it has been demonstrated that the vascular functionality of tumors is the primary target of HESW tumor therapy [53,157]. Exposure of tumors with HESW causes a temporary decrease in TBF resulting in a metabolic inactivation and acidification [155,157]. The modulatory effects of HESW on TBF may be used to overcome the limited efficacy of other treatment modalities. For instance, a threefold increase of the intra tumor concentration of systemically given tumor necrosis factor alpha (TNF-α) was achieved after HESW tumor treatment [28]. Moreover, the HESW induced decrease of TBF may probably improve the efficacy of thermotherapy. Monitoring the effects on TBF of (repeated) HESW exposure(s) is therefore of importance in order to improve the efficacy of HESW treatments, not only as monotherapy but also in combination with other therapies. A 24 hours time interval was chosen because we wanted to investigated the effects of a second HESW treatment after functional recovery of the TBF.

Several methods can be used to measure blood flow and tissue perfusion, either directly or indirectly [1]. Among the methods developed to measure TBF indirectly, radiolabeled and MRS detectable tracers are most commonly used. There are several advantages of MRS based methods above the use of radiolabeled tracers [44]. First of all MRS is nondestructive and relatively non-invasive. Secondly, stable isotopes (e.g. deuterium or fluorine) are used, eliminating problems of radiation exposure and special tracer handling. Finally, concurrent ^{1}H and ^{31}P MRS measurements can be performed, evaluating tissue metabolism. On the other hand, the main disadvantage of this technique is that it requires specialized and expensive equipment. In the present study we used the deuterium clearance method to calculate TBF at various time points after successive HESW exposures. In an earlier study we already demonstrated that in the NU-1 tumor this method gives reproducible deuterium outflow curves after repeated intra-tumoral D_2O injections, independent of the number of injection sites [157]. Here we demonstrate that a second HESW application of this NU-1 tumor result in a decrease in tumor blood flow which is statistically not different from the effect on TBF seen after the first HESW exposure. Both HESW exposures resulted in a significant decrease of TBF 2 hours after therapy, followed by normalization to pretreatment values within 16 hours. The extent and duration of the decrease in TBF after the first HESW administration were comparable with those described earlier [157].

However the absolute TBF flow values of the NU-1 tumors used in this study were much lower than found earlier [157] Several reasons can be taken into consideration for this major discrepancy First, there are major differences in tumor doubling time between the early passages used now and the late passages used earlier (8 and 3 5 days respectively) The lower tumor doubling time of these early passages of the NU-1 tumor might well be representative for a less well developed vascular system Secondly, since the MRS surface coil used in the present study was bigger than in our used earlier, the tumors needed to grow to significant higher volumes compared to the aforementioned study For other xenografts it has been demonstrated that TBF values correlate with tumor-volume, the bigger the tumor the lower the TBF [89] Finally, in contrast to our earlier study, D_2O clearance curves were best fitted using a one compartment model For the RIF tumor it has been demonstrated that TBF values, calculated using a mono-compartment model were significant lower compared to the TBF values calculated from the same clearance curves, using a two compartment model [77]

Earlier studies, using different tumor models, revealed that the antitumor effects of HESW could be enhanced by repeated HESW tumor treatments and that shortening of the interval between subsequent HESW treatments leads to more effective tumor growth inhibition [121 171] Our present TBF study rationalizes the shortening of the time interval between HESW exposure towards 2 3 hours Reperfusion of the HESW exposed tumor can not occur and the prolonged ischemia will induce more cell death Denekamp et al reported for the SA F mouse tumor that 15 hours of ischemia was required to obtain local cure of the tumor Assuming that such a long time period will also be necessary for other tumors, this would imply that 5 6 successive HESW treatments should be given to achieve sufficient ischemia time to provoke complete local tumor regression [31]

Optimalization of time schedules time schedules for HESW treatment in combination with other therapies, e g systemically given drugs (chemotherapy or BRMs), based on this study, will be more difficult Recently we demonstrated that a threefold increase in the intra-tumor concentration of systemically given TNF-α can be achieved after one HESW tumor treatment [28] Yet it is not known to what extent TBF must be recovered before a second treatment of HESW in combination with systemically given drugs would only be effective It is obvious that drugs need to have access to the tumor before the selective shut down of the tumor vasculature will result in increased intra tumoral drug levels

In conclusion, it becomes clear that HESW are capable to damage selectively the tumor vasculature It is tempting to speculate that this HESW induced decrease of tumor blood flow will be able to rule out problems of inadequate drug uptake and non optimal distribution in the tumor The potency of HESW to increase the efficacy of systemic therapies by selective temporary changes in TBF will possible determine its clinical application

Chapter 7

SUMMARY AND CONCLUSIONS

SUMMARY AND CONCLUSIONS

The application of magnetic resonance based techniques has expanded in medical science in the past few years. In particular, magnetic resonance imaging (MRI) has become a routine examination in clinical medicine, but magnetic resonance spectroscopy (MRS) is still in its experimental setting although several studies have demonstrated that MRS can be used to monitor biochemical processes. Several applications for MRS like improvement of diagnosis by providing metabolic markers, monitoring the response to therapy by MRS detectable metabolites and monitoring the pharmacokinetics of cancer drugs are of particular clinical interest. This thesis describes experimental studies on the potential applications of MRS in urological oncology. In chapter 2, 3, and 4 *in vitro* MRS studies are described to determine the possible value for MRS in diagnosis and staging of prostate cancer. In chapter 5 and 6 *in vivo* MRS was used to monitor the effects of HESW as anti-tumor therapy in order to elucidate its working mechanism and to provide a rational for improving the current treatment schedules of this new experimental anti-cancer therapy.

Chapter 2 describes an *in vitro* ^{1}H and ^{31}P MRS study of perchloric acid extracts of human prostate tissue obtained by transurethral resection. This included tissue of patients with benign prostatic hyperplasia (BPH), prostatic adenocarcinoma and non-malignant tissue (i.e no sign of histological BPH or cancer). Prominent resonances in the MR spectra could be assigned and were quantified. The citrate / lactate, citrate / total choline, phosphocholine / total creatine, choline / total creatine, alanine / total creatine, phosphoethanolamine / total phosphate, phosphocholine / total phosphate and glycerophosphoethanolamine / total phosphate ratios were statistically different for the prostate cancer samples as compared to the BPH specimens. We therefore concluded, that MRS may be of additional use in the diagnosis of prostate cancer.

In ***chapter 3*** we investigated whether the differences in biological potential of rat prostate cancers correlated with changes in metabolic profiles. ^{1}H and ^{31}P MR spectra were acquired from perchloric acid extracts of seven Dunning R-3327 rat prostate tumor sublines. Several metabolic ratios, e.g. phosphocholine / total phosphate, choline / total creatine and inositol / total creatine did not correlated specifically with any of the tumor biological characteristics. However, in terms of these ratios we could discriminate between the well differentiated, non-metastatic and hormone dependent sublines versus the poorly differentiated or anaplastic, metastatic and hormone independent sublines. The glycerophosphoethanolamine / total phosphate, glycerophospho-choline / total phosphate and phosphocreatine / total phosphate ratios correlated with differentiation grade and the difference in glycerophosphoryl-glycerol / total phosphate ratio between metastatic and non-metastatic sublines was

highly significant No correlation between hormonal sensitivity and any of the MRS detectable metabolites were found Based on this study we concluded that for rat Dunning prostate tumors biological parameters correlated with metabolic profiles
To extend these observations for human prostate cancer, four well established human prostate cancer cell lines were studied with ^{1}H MRS to compare differences in metabolic content with tumor biological behaviour In ***chapter 4*** we demonstrate that, despite unique metabolic profiles, the relative creatine and citrate levels can be used to discriminate the androgen dependent LNCaP cell line from the androgen independent DU-145, TSU and PC-3

Chapter 5 describes how *in vivo* MRS can be used to investigate the effects of HESW exposure of NU-1 tumors on particularly tumor blood flow (TBF) Also changes in metabolism using multinuclear $^{1}H/^{2}H/^{31}P$ MRS were thus studied By monitoring deuterium washout, we could demonstrate that a dramatic reduction in TBF is seen if the tumor is subjected to HESW In addition, the concomitant monitoring of ^{1}H and ^{31}P MRS showed a transient acidification of the tumor and an increase in the lactate concentration All changes were temporary and recovered to pretreatment levels These studies support the hypothesis that the functional vascularity is an important target of HESW exposure
Since the anti-tumor effects of HESW are probably associated with the extend and duration of the decrease of TBF after successive HESW exposures we evaluated in ***chapter 6*** the effects of repeated HESW tumor administration on TBF We demonstrated that a second HESW exposure, administrated after functional recovery of the tumor, resulted in a decrease in TBF which is not different from the effect on TBF seen after the first HESW exposure Both HESW exposures resulted in a significant decrease of TBF 2 hours after therapy, followed by normalization to pretreatment values within 16 hours The extent and duration of the decrease in TBF after the first HESW administration were comparable with those described in chapter 5 These observations provide a rational to shorten the time interval between HESW mono-treatments to 2-3 hours

Samenvatting en conclusies

Het gebruik van kernspinresonantie technieken in de medische wetenschap heeft in de afgelopen jaren een explosieve groei doorgemaakt In het bijzonder is de beeldvorming met kernspin resonantie, ook wel magnetische resonantie imaging (MRI) genoemd, een routine afbeeldingstechniek in de kliniek geworden De magnetische kernspin resonantie spectroscopie (MRS), met behulp waarvan stofwisselingsprocessen in weefsels bestudeerd kunnen worden, wordt voornamelijk voor research doeleinden gebruikt Verschillende toepassingsmogelijkheden voor MRS zoals a verbetering van diagnostiek met behulp van metabole markers b evaluatie van therapie c farmacokinetiek studies van (kanker) medicamenten kunnen van waarde zijn voor de kliniek
In dit proefschrift worden experimentele studies beschreven, om de waarde van MRS voor de urologische oncologie te bepalen In hoofdstuk 2, 3 en 4 worden *in vitro* MRS studies beschreven, waarin getracht wordt de waarde van MRS voor de diagnostiek van prostaataandoeningen, in het bijzonder prostaatkanker, te bepalen In hoofdstuk 5 en 6 worden *in vivo* MRS studies beschreven ter evaluatie van het werkingsmechanisme van HESW als anti-tumor therapie

In hoofdstuk 1 wordt een algemene korte inleiding over de algemene principes en toepassingsmogelijkheden van *in vitro* en *in vivo* MRS voor de oncologische research gegeven

Hoofdstuk 2 beschrijft een *in vitro* ^{1}H en ^{31}P MRS studie van perchloorzuur (PCA) extracten van transurethraal resectie materiaal specifiek voor de normale prostaat, benigne prostaat hyperplasie (BPH) en adenocarcinoom van de prostaat De meest uitgesproken resonanties in de MR spectra werden geidentificeerd en gekwantificeerd De volgende ratio's citraat/lactaat, citraat/totaal choline, fosfocholine/totaal creatine, choline/totaal creatine, alanine/totaal creatine, fosfoethanolamine/totaal fosfaat, fosfocholine/totaal fosfaat en glycerofosfoethanolamine/totaal fosfaat waren verschillend bij BPH in vergelijking met die bij het adenocarcinoom Op basis van deze resultaten zijn we tot de conclusie gekomen, dat MRS mogelijk van waarde kan zijn in de diagnostiek van prostaat kanker

In hoofdstuk 3 hebben we met behulp van het Dunning prostaat tumor model onderzocht, of verschillen in tumor biologisch gedrag correleren met veranderingen in metabool profiel Een ^{1}H en ^{31}P MRS studie van PCA extracten van zeven verschillende sublijnen werd uitgevoerd Dezelfde metabolieten als in de humane spectra werden geidentificeerd en gekwantificeerd Verschillende ratio's fosfocholine/totaal fosfaat, choline/totaal creatine en inositol/totaal creatine, konden

worden gebruikt om de agressieve sublijnen (slecht gedifferentieerd, metastaserend en hormonaal onafhankelijk) van de relatief benigne sublijnen te onderscheiden De glycerofosfoethanolamine/totaal fosfaat, glycerofosfocholine/totaal fosfaat en fosfocreatine/totaal fosfaat ratio's waren significant verschillend in de goed en matig gedifferentieerde sublijnen in vergelijking met de slecht gedifferentieerde en anaplastische sublijnen De hoogte van de glycerofosforylglycerol/totaal fosfaat ratio correleerde met uitzaaiend vermogen van de Dunning sublijnen In deze dierexperimentele studie kon geen correlatie gevonden worden tussen hormonale response en de gekwantificeerde metabolieten

In hoofdstuk 4 hebben we onderzocht, of de correlatie tussen biologisch gedrag en metabool profiel, zoals die in hoofdstuk 3 gevonden werd, ook voor humane prostaat kanker geldt Hiertoe werden PCA extracten van vier humane cellijnen met ^{1}H MRS onderzocht De resultaten van deze studie laten zien, dat de hormonaal afhankelijke LNCaP cellen relatief meer creatine bevatten dan de andere drie hormonale onafhankelijke cellijnen Tevens suggereren de resultaten, dat het citraat gehalte van LNCaP cellen hoger is dan dat van de DU 145, TSU PR1 en PC-3
Op basis van de in hoofdstuk 3 en 4 beschreven studies concluderen we, dat het met behulp van MRS mogelijk is om prostaat tumoren met verschillend biologisch gedrag van elkaar te onderscheiden

Om meer inzicht te verkrijgen in het werkingsmechanisme van hoog energetische schokgolven (HESG) als anti-tumor therapie werd *in vivo* MRS gebruikt Deze techniek verschaft informatie over metabole veranderingen in viabele tumorcellen, welke het doel zijn van de HESG behandeling
In hoofdstuk 5 zijn de effecten van een eenmalige HESG blootstelling op het tumorcelmetabolisme en de tumor bloed doorstroming (TBF) beschreven Een dramatische, maar tijdelijke, verlaging van de tumor doorbloeding werd gezien In hetzelfde tijdsinterval werd met behulp van ^{1}H en ^{31}P MRS een daling van de pH en een stijging van het melkzuur gehalte gezien Daar we, mede op basis van deze MRS studie, mogen stellen, dat de doorbloeding van de tumor waarschijnlijk het voornaamste aangrijpingspunt van HESG therapie is, is het in beeld brengen van de mate en de duur van de gestoorde TBF na herhaalde HESG blootstellingen belangrijk voor de ontwikkeling en verbetering van therapie protocollen Het doel van de in hoofdstuk 6 beschreven studie was, om de effecten op de TBF na herhaalde HESG blootstelling te evalueren In dit hoofdstuk laten we zien, dat een tweede HESG blootstelling, 24 uur na de eerste, resulteert in een verlaging van de TBF, welke niet verschilt van het effect op de TBF na de eerste keer Twee uur na beide HESG blootstellingen wordt een significant verlaagde TBF gezien, welke binnen zestien uur herstelt naar normale waarden Op grond van deze resultaten concluderen we, dat het tijdsinterval tussen opeenvolgende HESG behandelingen verlaagd kan worden tot 2 a 3 uur

PERSPECTIVES

MRS as diagnostic tool in prostate cancer

Nuclear magnetic resonance based techniques provide new diagnostic tools for clinical use. The development of endorectal MRI surface coils improved the detection and staging of prostate cancer. Likewise, MRS of the prostate can be performed (figure 1: MRI/MRS of prostate of young volunteer). Since little is known about the biochemical content of the prostate, *in vitro* MRS studies were performed in order to gain insight in the metabolic content. Subsequently, the potential value of MRS in improving diagnosis of prostate malignancies can be determined. Moreover, using different prostate tumor models systems, differences in metabolic content of prostate tumors can be related to their different tumor biological potential. From chapter 2-4 we can conclude that there are several potential markers for prostate cancer, e.g., citrate and (phospho)choline. Moreover, our results suggest that prostate tumors with different biological potential can be identified using MRS.

In vivo ^{1}H MRS studies of the prostate with endorectal coils continue to support the importance of citrate as marker of malignancy in the prostate. In an ongoing *in vivo* MRS study of the prostate not only citrate but also choline appear to be useful in discriminating BPH from adenocarcinoma of the prostate.[62] However, the results of these single volume localization studies may be ambiguous because of the known heterogeneity of prostate cancer. Spectroscopic imaging techniques may overcome these problems and may enable visualization of the spatial distribution of citrate, choline or other metabolites. If spectroscopic imaging of small volumes of less then 1 cc becomes feasible, metabolic maps of the prostate will probably help to delineate the extension of the tumors and thus allow better local staging. Secondly, in the future prognostic information about the biological behaviour of the lesion may be derived from MRS.

The question "Is there a clinical role for MRS in detection and staging of prostate cancer" remains to be solved. Although multi-center trials are clearly needed to solve that question, this thesis indicates that MRS will play a role in the diagnosis of prostate diseases, i.e. BPH and prostate cancer.

MRS monitoring HESW anti-tumor therapy

A number of years ago Oosterhof and Smits wrote "We do not know whether high energy shock waves will ever become clinically applicable in (urological) oncology.".[122,156] This thesis will not answer that particular question, but based on the MRS studies described in chapter 5 and 6 we further improved our knowledge about the mode of action of HESW in tumor therapy. We concluded that one of the main targets of HESW is the functional vascularity of the tumor.

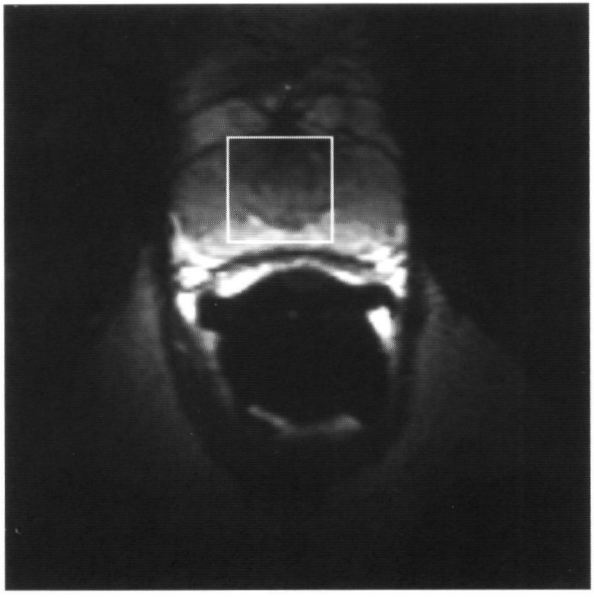

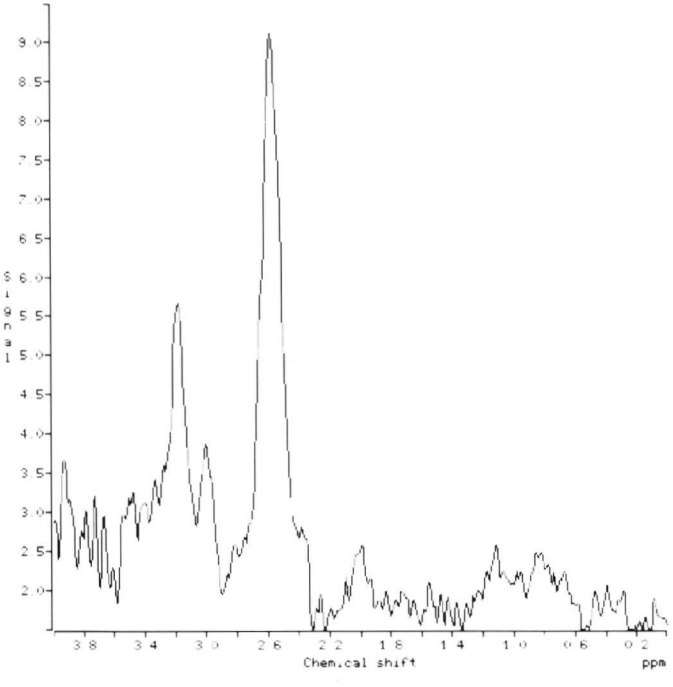

Figure 1. MRI / MRS of the prostate of a young volunteer.

Based on these studies treatment schedules of HESW as monotherapy can be improved. Hoshi et al already suggested in 1991 that a decrease in time interval between HESW exposures might be beneficial[67] Our studies described in chapter 6 rationalizes a decrease to 2-3 hours

Based on the study described in chapter 5 we recently hypothesized that the concentration of systemically given drugs can be locally increased by the application of HESW [28] Until now several attempts have been made to ***increase*** TBF in order to overcome poor drug delivery due to heterogeneous blood supply [71] We however, demonstrated that a HESW induced ***decrease*** in tumor blood flow results in an increased local concentration of the systemically given drug [28] Thus lower doses of systemically given drugs, e g chemotherapeutics, with less general toxicity, may be necessary to achieve similar antitumor efficacy In a recent pilot study, combining low dose systemically given TNF-α with HESW, we achieved a higher percentage of complete responses in the combination group as compared to both treatments alone (unpublished results)

Till now, MRS has only been used in urological oncology in an experimental setting to monitor alterations in metabolism after therapy Currently, there have been only a limited number of, non-urological, *in vivo* MRS studies published using MRS for therapy evaluation Whether this technique will be applicable for therapy evaluation in urological oncology is not known yet The endorectal MRS prostate probe, currently experimentally used for diagnosis, might also be benificial for (hormonal) therapy evaluation Future will learn whether MRS will become an established tool in diagnosis and therapy monitoring in urological oncology

References

1 **Ackerman J.J.**, Ewy C S , Becker N N , Shalwitz R A Deuterium nuclear magnetic resonance measurements of blood flow and tissue perfusion employing 2H2O as a freely diffusible tracer *Proc Natl Acad Sci USA* **84**, 4099-4102, 1987

2 **Agris P.F.**, Campbell I D Proton nuclear magnetic resonance of intact Fried leukemia cells phosphorylcholine increase during differentiation *Science*, **216**, 1325-1327, 1982

3 **Appelgren K.L.** Methods of recording tumor blood flow In Peterson, H-I , ed Tumor Blood Circulation Boca Raton CRC press, 1979 87-101

4 **Baldwin J.J.** and Cornatzer W E Rat kidney glycerylphosphoryl choline diesterase *Biophys Acta*, **164** 195-204, 1968

5 **Ban N.**, Moriyasu F , Tamada T , Kawasaki T , Soh Y , Nakamura T , Nishida O In vivo P-31 MR spectroscopic study of cirrhotic liver using a whole body imager *Nippon Shokakibyo Gakkai Zasshi*, **84**, 2551-2557, 1987

6 **Barzilai A.**, Horowitz A , Geier A , Degani H Phosphate metabolites and steroid hormone receptors of benign and malignant breast tumors A nuclear magnetic resonance study *Cancer*, **67**, 2919-2925, 1991

7 **Bell J.D.**, Gadian D G , Preece N E Nmr studies of drug metabolism and disposition *Eur J Drug Metab Pharmacokinet* , **15**, 127-133, 1990

8 **Bendall M.R.**, Pegg D T Theoretical description of depth pulse sequences, on and off resonance, including improvements and extensions thereof *Magn Reson Med* **2**, 91-113, 1985

9 **Bloch F.**, Hansen W W , Pckard M E Nuclear induction *Physiol Rev* , **69**, 127, 1946

10 **Blondet P.** Albrand J D , von Kienlin M , Decorps M Use of rotating-phase DANTE pulses for in vivo proton NMR spectral editing with a single irradiation facility *J Magn Reson* **71**, 342-346, 1987

11 **Boring C.C.**, Squires I S and Tong T Cancer statistics 1992 *Ca*, **42**, 19-38, 1992

12 **Bourgeois D.**, Decorps M , Remy C , Benabid A L High-flux signals and spatial localization in high-resolution ^{1}H spectroscopy with surface coils *Magn Reson Med* , **11**, 275-281, 1989

13 **Brinkman G.**, Melchert U , Forger K , Wunsch-Binder F , Heidemann H , Engmann R In vivo phosphorus magnetic resonance spectroscopy of liver diseases *Fortschr Geb Rontgenstr Nuklearmed Erganzungsband*, **153**, 204-208, 1990

14 **Brown T.R.**, Graham R A , Szwergold B S , Thoma W J and Meyer R A Phosphorylated metabolites in tumors, tissues, and cell lines *Ann N Y Acad Sci* , **508**, 229-240, 1987

15 **Bryant D.J.**, Bydder G M , Case H A , Collins A G , Cox I J , Makepeace A , Pennock J M Use of phosphorus-31 MR spectroscopy to monitor response to chemotherapy in non-Hodgkin lymphoma *J Comput Assist Tomogr* , **12**, 770-774, 1988

16 **Bussemakers M.J.G.**, van Moorselaar R J A , Giroldi L A , Ichikawa T , Isaacs J T , Takeichi M Debruyne F M J , Schalken J A , Decreased expression of E cadherin in the progression of rat prostate cancer *Cancer Res* , **52**, 2916-2922, 1992

17 **Cadoux-Hudson T.A.D.**, Blackledge M J , Rajagopalan B , Taylor D J ,

Radda G K Human primary brain tumour metabolism in vivo a phosphorus magnetic resonance spectroscopy study *Br J Cancer*, **60**, 430 436 1989

18 **Carpinelli G.** Podo F , Di Vito M , Proietti E Gessanni S , Belardelli F Modulations of glycerophosphorylcholine and phosphorylcholine in Friend erythroleukemia cells upon in vitro-induced erythroid differentiation a ^{31}P NMR study *FEBS Lett* **176** 88 92, 1984

19 **Catalona W.J.**, Scott W W Carcinoma of the prostate In Walsh P C Gittes, R F , Perlmutter, A D , and Stamey, T A (eds) *Campbells Urology*, **2** 1463-1534 (Philadelphia W B Saunders) 1986

20 **Catalona W.J.**, Smith D S , Ratliff T L Dodds K M Coplen D E , Yaun J J J , Petros J A and Andriole G L Measurement of prostate specific antigen in serum as a screening test for prostate cancer *N Engl J Med* , **324**, 1156-1161, 1991

21 **Cohen J.S.**, Lyon R C , Chen C , Fautimo P J , Batist G , Shoemaker M , Rubalcaba E , Cowan K H Differences in phosphate metabolic levels in drug sensitive and -resistant human breast cancer cells lines determined by ^{31}P magnetic resonance spectroscopy *Cancer Res* **46**, 4087-4090, 1986

22 **Cohen J.S.** Phospholipid and energy metabolism of cancer cells monitored by ^{31}P magnetic resonance spectroscopy possible clinical significance *Mayo Clin Proc* , **63**, 1199 1207, 1988

23 **Cooper J.F.**, Farid I The role of citric acid in the physiology of the prostate III Lactate/citrate ratios in benign and malignant prostatic homogenates as an index of prostatic malignancy *J Urol* , **92** 553, 1964

24 **Corbett R.J.T.**, Nunnally R L , Giovanella B C , Antich P P Characterization of the ^{31}P nuclear magnetic resonance spectrum from human melanoma tumors implanted in nude mice *Cancer Res* , **47**, 5065-5069, 1987

25 **Cornel E.B.**, Smits G A H J , Oosterhof G O N , Karthaus H F M , Debruyne F M J , Schalken J A and Heerschap A Characterization of human prostate cancer, benign prostatic hyperplasia and normal prostate by in vitro ^{1}H and ^{31}P magnetic resonance spectroscopy *J Urol* **150**, 2019-2024, 1993

26 **Cornel E.B.**, Smits G A H J , Schalken J A , Debruyne F M J and Oosterhof G O N Biological effects of high energy shock waves in different tumor model systems *Forum*, **4**, 4-14, 1994 (review)

27 **Cornel E.B.**, Heerschap A , Smits G A H J Oosterhof G O N , Debruyne F M J , and Schalken, J A Alterations in metabolism within the Dunning R-3327 rat prostate tumor model discriminative for different tumor biological behavior a ^{1}H and ^{31}P magnetic resonance spectroscopy study *Prostate in press*

28 **Cornel E.B.**, Oosterwijk E , van de Streek J D , Grutters G Debruyne F M J , Schalken J A , Oosterhof G O N High energy shock waves induced increase in the local concentration of systemically given TNF-α *submitted*

29 **Costello, L.C.**, Littleton, G K and Franklin, R B Regulation of citrate-related metabolism in normal and neoplastic prostate *In endocrine control in neoplasia* edited by R K Sharma and W F Criss New York Raven press 303 314, 1978

30 **Costello, L.C.** and Franklin, R B Prostate epithelial cells utilize glucose and aspartate as carbon sources for net citrate production *Prostate*, **15**, 335, 1989

31 **Costello L.C.**, Franklin R B Concepts of citrate production and secretion by prostate I Metabolic relationships *Prostate*, **18**, 25-46, 1991

32 **Daly P.F.**, Lyon R C , Faustino P J , and Cohen J S Phospholipid metabolism in cancer cells monitored by ^{31}P NMR Spectroscopy *J Biol Chem* , **31**, 14875 1987

33 **Daly P.F.**, Cohen J S Magnetic resonance spectroscopy of tumors and the potential in vivo clinical applications a review *Cancer Res* , **49**, 770-779, 1989

34 **Debus J.**, Peschke P , Hahn E W , Lorenz W J , Lorenz A , Ifflander H , Zabel H J , van Kaick G , Pfeiler M Treatment of the Dunning tumor R3327 AT1 with pulsed high energy ultrasound shock waves, (PHEUS) growth delay and histo-orphologic changes *J Urol* , **146**, 1143-1146, 1991

35 **Degani H.**, Horowitz A , Itzchak I Breast tumors evaluation with ^{31}P NMR spectroscopy *Radiology*, **161**, 53-55, 1986

36 **Denekamp J.** Hill S A , Hobson, B Vascular occlusion and tumour cell death *Eur J Cancer Clin Oncol* **19**, 271-275, 1983

37 **Delius M.**, Weiss N , Gambihler S , Goetz A , Brendel W Tumor therapy with shock waves requires modified lithotripter shock waves *Naturwissenschaften*, **76**, 573-574 1989

38 **Delius M.**, Denk R , Berding C , Liebich H-G , Jordan M Brendel W Biological effects of shock waves cavitation by shock waves in piglet liver *Ultrasound Med Biol* , **16**, 467-472, 1990

39 **Dewhirst M.W.**, Sostman H D , Leopold K A , Charles H C , Moore D , Burn R A Tucker J A , Harrelson J M , Oleson J R Soft-tissue sarcomas MR imaging and MR spectroscopy for prognosis and therapy monitoring *Radiology*, **174**, 847-853, 1990

40 **Evanochko W.T.**, Sakai T T , NG, T C Rama Krishna N , Kim H D , Zeidler R B Ghanta V K , Brockman R W , Schiffer L M , Braunschweiger P G , Glickson J D NMR study of in vivo RIF 1 tumors analysis of perchloric acid extracts and identification of ^{1}H, ^{31}P and ^{13}C resonances *Biochim Biophys Acta*, **805**, 104-116, 1984

41 **Evelhoch J.L.**, Keller N A , Corbett T H Response-specific adriamycin sensitivity markers provided by in vivo ^{31}P nuclear magnetic resonance spectroscopy in murine mammary adenocarcinomas *Cancer Res* , **47**, 3396-3401, 1987

42 **Evelhoch J.L.**, Bissery M-C , Chabot G G , Simpson N E , McCoy C L , Heilbrun L K , Corbett T H Flavone acetic acid (NSC 347512)-induced modulation of murine tumor physiology monitored by in vivo nuclear magnetic resonance spectroscopy *Cancer Res* **48**, 4749 4755, 1988

43 **Evelhoch J.L.**, McCoy C L , Giri B P A method for direct in vivo measurements of drug concentration from a single ^{2}H NMR spectrum *Magn Reson Med* **9**, 402-410, 1989

44 **Evelhoch, J.L.** Measurement of tumor blood flow by deuterium NMR and the effects of modifiers *NMR in Biomed* , **5**, 290-295, 1992

45 **Evelhoch J.L.**, Larcomb-McDouall J B , Mattiello J , Simpson N E

Measurement of relative regional tumor blood flow in mice by deuterium NMR imaging *Magn Reson Med* , **24,** 42-52, 1992

46 **Fowler A.H.**, Pappas A A , Holder J C , Finkbeiner A E , Dalrymple G V , Mullins M S , Sprigg J R , and Komoroski R A Differentiation of human prostate cancer from benign hypertrophy by in vitro ^{1}H NMR *Magn Reson Med* , **25**, 140-147, 1992

47 **Foxall D.L.**, Cohen J S NMR studies of perfused cells *J Magn Reson* , **52**, 346-349, 1983

48 **Francis I.R.,** Chenevert T L , Gubin B , Collomb L , Ensminger W , Walker-Andrews S , Glazer G M Malignant hepatic tumors P-31 MR spectroscopy with one-dimensional chemical shift imaging *Radiology*, **180**, 341 344, 1991

49 **Franklin R.B.**, Costello L C , Littleton G K Citrate uptake and oxidation by fragments of rat ventral prostate *Enzyme*, **22**, 45-51, 1977

50 **Gadian D.G.** Nuclear magnetic resonance and its application to living sys tems Clarendon Press, Oxford, 1982

51 **Gadian** D G , Radda G K , Ross B D et al Examination of a myopathy by phosphorus nuclear magnetic resonance *Lancet*, **2**, 774-775, 1981

52 **Galons J.-P** , Fantini J , Vion-Dury J , Cozzone P J , Canioni P Metabolic changes in undifferentiated and differentiated human colon adenocarcinoma cells studied by multinuclear magnetic resonance spectroscopy *Biochimie*, **71**, 949-961, 1989

53 **Gamarra F.**, Spelsberg F Kuhnle G E H , Goetz A E High energy shock waves induce blood flow reduction in tumors *Cancer Res* , **53** 1590-1595, 1993

54 **Gibson S.L.,** Ceckler T L , Bryant R G , Hilf R Effects of laser photodynamic therapy on tumor phosphate levels and pH assessed by ^{31}P-NMR spectroscopy *Cancer Biochem Biophys* , **10,** 319-328, 1989

55 **Glaholm J.**, Leach M O , Collins D J Mansi J , Sharp J C , Madden A , Smith I E , McCready J R In vivo ^{31}P magnetic spectroscopy for monitoring treatment response in breast cancer *Lancet*, **1**, 1326-1327, 1989

56 **Glickson J.D.**, Wehrle J P , Rajan S S , Li S J , Steen R G NMR spectroscopy of tumors In *NMR, principles and applications to biomedical research*, 255 - 309 Pettegrew J W (ed) Springer-Verlag, New York, 1990

57 **Glonek T.** and Kopp S J Ex vivo P-31nmr of lens, cornea, heart, and brain *Magn Reson Imaging*, **3**, 359-376, 1985

58 **Griffiths J.R.** Are cancer cells acidic? *Br J Cancer*, **64,** 425-427, 1991

59 **Haase A.**, Frahm J , Haenicke W , Matthaei D ^{1}H NMR chemical shift selective (CHESS) imaging *Phys Med Biol* , **30,** 341-344, 1985

60 **Hanaoka H.**, Yoshioka Y , Ito I , Niito K , Yasuda N In vitro characterization of lung cancers by the use of ^{1}H nuclear magnetic resonance spectroscopy of tissue extracts and discriminant factor analyses *Magn Reson Med* , **29,** 436-440, 1993

61 **Hanstock C.C.**, Bendall M R , Hetherington H P , Boisvert D P , Allen P S Localized in vivo proton spectroscopy using depth pulse spectral editing *J Magn Reson* , **71,** 349-354, 1987

62 **Heerschap A.**, de Jager G , de Koster A Barentz J , de la Rosette J , Debruyne F , Ruijs J ^{1}H MRS of pros-

tate pathology *Book of abstracts annual meeting Society of Magnetic Resonance in Medicine*, New York 14-20 August 1993, page 213

63 **Hetherington H.P.**, Avison M J , Schulman R G ^{1}H homonuclear editing of rat brain using semiselective pulses *Proc Natl Acad Sci USA*, **82,** 3115-3118, 1985

64 **Holmes R.P.** Yeaman L I Li W-J , Hart L J, Wallen C A Woodruff R D , McCullough D L The combined effect of shock waves and cisplatin therapy on rat prostate tumors *J Urol* **144** 159-163, 1990

65 **Hore P.J.** Solvent suppression in Fourier transform nuclear magnetic resonance *J Magn Reson* , **54,** 539-542, 1983

66 **Horoszewicz J.S.**, Leong S S , Kawinski E , Karr J P , Rosenthal H , Chu T M , Mirand E A , Murphy G P LNCaP model of human prostatic carcinoma *Cancer Res* , **43**, 1809-1818, 1983

67 **Hoshi S.**, Orikasa S , Kuwahara M , Suzuki K , Yoshikawa K , Saitoh S Ohyama C , Satoh M , Kawamura S , Nose M High energy under water shock wave treatment on implanted urinary bladder cancer in rabbits *J Urol* , **146,** 439-443 1991

68 **Hwang Y.**, Kim S-G , Evelhoch J L , Seyedsadr M , Ackerman J J H Modulation of murine radiation-induced fibrosarcoma-1 tumor metabolism and blood flow in situ via glucose and mannitol administration monitored by ^{31}P and ^{2}H nuclear magnetic resonance spectroscopy *Cancer Res* , **51,** 3108-3118, 1991

69 **Iizumi T.**, Yazaki T , Kanoh S , Kondo I , Koiso K Establishment of a new prostatic carcinoma cell line (TSU-PR1) *J Urol* , **137** 1304-1306, 1987

70 **Isaacs J.T.**, Hukku B Nonrandom involvement of chromosome 4 in the progression of rat prostatic cancer *Prostate*, **13**, 165-188, 1988

71 **Jain R.K.** Delivery of novel therapeutic agents in tumours physiological barriers and strategies *J Natl Cancer Inst* , **81**, 570-576 1989

72 **Kaighn M.E.**, Narayan K S , Ohnuki Y Lechner J F , Jones L W Establishment and characterization of a human prostatic carcinoma cell line (PC-3) *Invest Urol* , **17**, 16-23, 1979

73 **Karczmar G.S.**, Meyerhof D J , Boska M D , Hubesch B , Poole J , Matson G B , Valone F , Weiner M W P-31 spectroscopy study of response of superficial human tumors to therapy *Radiology*, **179**, 149-153, 1991

74 **Kasimos J.N.**, Merchant T E , Gierke L W , Glonek T ^{31}P magnetic resonance spectroscopy of human colon cancer *Cancer Res* , **50**, 527-532, 1990

75 **Kennedy E.P.**, Weiss S B The function of cytidine coenzymes in the biosynthesis of phospholipids *J Biol Chem* , **222**, 193-214, 1956

76 **Kim S-G.**, Ackerman J J H Multicompartment analysis of blood flow and tissue perfusion employing D_2O as a freely diffussible tracer a novel deuterium NMR technique demonstrated via application with murine RIF-1 tumors *Magn Reson Med* , **8,** 410 426, 1988

77 **Kim S-G.**, Ackerman, J J H Quantitative determination of tumor blood flow and perfusion via deuterium nuclear magnetic resonance spectroscopy in mice *Cancer Res* **48**, 3449-3453, 1988

78 **Kim S-G** , Ackerman, J J H Quantification of regional blood flow by monitoring of exogenous tracer via

nuclear magnetic resonance spectroscopy *Magn Reson Med* , **14**, 266-282, 1990

79 **Kintner D.**, Fitzpatrick J H Louie L A and Gilboe D D Cerebral oxygen and energy metabolism during and after 30 minutes of moderate hypoxia *Am J Physiol* , **247** 475-482 1984

80 **Kobayashi M.**, Lust W D and Passoneau J V Concentration of energy metabolism and cyclic nucleotides dur ing and after bilateral ischemia in the gerbil cerebral cortex *J Neurochem* , **29**, 53-59, 1977

81 **Koutcher J.A.**, Ballon D , Graham M , Healey J H Casper E S , Heelan R , Gerweck L E ^{31}P NMR spectra of extremity sarcomas diversity of metabolic profiles and changes in response to chemotherapy *Magn Reson Med* , **16**, 19-34, 1990

82 **Kurhanewicz J.**, Dahiya R , Macdonald J M , Chang L H , James T L , Narayan P Citrate alterations in primary and metastatic human prostatic adenocarcinomas ^{1}H magnetic resonance spectroscopy and biochemical study *Magn Reson Med* , **29**, 149-157 1993

83 **Larcombe-Mc Douall J.B.**, Evelhoch, J L Deuterium nuclear magnetic resonance imaging of tracer distribution in D_2O clearance measurements of tumor blood flow in mice *Cancer Res* , **50**, 363-369, 1990

84 **Leach M.**, Le Moyec L , Podo F MRS of tumours basic principles In Magnetic resonance spectroscopy in biology and medicine page 295-344, edited by de Certaines J D , Bovee W M M J and Podo F Pergamon Press, 1992

85 **Lee K-E.** Smith P Cockett A T K Influence of high energy shock waves and cisplatin on antitumor effect in murine bladder cancer *Invest Urol* **5**, 440-444, 1990

86 **Li S.-J.** Wehrle J P , Rajan S S , Steen R G , Glickson J D , Hilton J Response of radiation-induced fibrosarcoma-1 in mice to cyclophosphamide monitored by in vivo ^{31}P nuclear magnetic resonance spectroscopy *Cancer Res* , **48**, 4736-4742, 1988

87 **Lilly M.B.**, Katholi C R , Ng T C Direct relationship between high energy phosphate content and bloodflow in thermally treated murine tumors *J Natl Cancer Inst* , **75**, 885-889, 1985

88 **Ling D.**, Lee J K T , Heiken J P , Balfe D M , Glazer H S , McClennan B L , Prostatic carcinoma and benign prostatic hyperplasia inability of MR imaging to distinguish between the two diseases *Radiology*, **158**, 103-107, 1986

89 **Lyng H.**, Skretting A , Rofstad E K Blood flow in six human melanoma xenograft lines with different growth characteristics *Cancer Res* **52**, 584-592, 1992

90 **Macdonald J.M.**, Kurhanewicz J , Dahiya R , Espanol M T , Chang L-H , Goldberg B , James T L , Narayan P Effect of glucose and confluency on phosphorus metabolites of perfused human prostatic adenocarcinoma cells as determined by ^{31}P MRS *Magn Reson Med* , **29**, 244-248, 1993

91 **Mafee M.F.**, Puklin J , Barany M , Cohen S , Wycliffe N MRI and in vivo proton spectroscopy of lesions of the globe *Sem Ultrasound, CT MR*, **9**, 428-442, 1988

92 **Malet-Martino M.C.**, Martino R Uses and limitations of nuclear magnetic resonance (NMR) spectroscopy in clinical pharmacokinetics *Clin Pharmacokinet* , **20**, 337-349, 1991

93 **Marberger H.**, Marberger E , Mann T , Lutwak-Mann C Citric acid in human prostatic secretion and metastasizing cancer of the prostate *Br Med J* , **1**, 835, 1962

94 **Marion D.** and Wuthrich K Application of phase sensitive two-dimensional correlated spectroscopy (cosy) for measurements of ^{1}H-^{1}H spin-spin coupling constants in proteins *Biochem Biophys Res Commun* , **113**, 967 974, 1983

95 **Maris J.M.**, Evans A E , McLaughlin A C , D'Angio G J , Bolinger L , Manos H , Chance B ^{31}P nuclear magnetic resonance spectroscopic investigation of human neuroblastoma in situ *N Engl J Med* , **312**, 1500-1505, 1985

96 **Maxwell R.J.**, Prysor-Jones R A , Jenkins J S , Griffiths J R Vasoactive intestinal peptide stimulates glycolysis in pituitary tumours ^{1}H NMR detection of lactate in vivo *Biochim Biophys Acta* , **968**, 86-90, 1988

97 **Meneses P.**, Para P , Glonek T ^{31}P NMR of tissue phospholipids a comparison of three tissue pre-treatment procedures *J Lipid Res* , **30**, 458 461, 1989

98 **Merchant T.E.**, Gierke L W , Meneses P , and Glonek T ^{31}P magnetic resonance spectroscopic profiles of neoplastic human breast tissues *Cancer Res* , **48**, 5112-5118, 1988

99 **Merchant T.E.**, Kasimos J N , deGraaf P W , Minsky, B D , Gierke L W , Glonek T phospholipid profiles of human colon cancer using ^{31}P magnetic resonance spectroscopy *Int J Colorectal Dis* , **6**, 121-126, 1991

100 **Merchant T.E.**, Meneses P , Gierke L W , Den Otter W , Glonek T ^{31}P magnetic resonance phospholipid profiles of neoplastic human breast tissues *Br J Cancer*, **63**, 693 698, 1991

101 **Merchant T.E.**, Nieuwenhuizen C W E A , de Graaf P W , Kievit H C E , den Otter W , Glonek T Clinical magnetic resonance spectroscopy of human breast disease *Invest Radiol* , **26**, 514-516, 1991

102 **Moreno A.**, Rey M , Montane J M , Alonso J , Arus C ^{1}H NMR spectroscopy of colon tumor and normal mucosal biopsies. Elevated taurine levels and reduced polyethyleneglycol absorption in tumors may have diagnostic significance *NMR Biomed* , **6**, 111-118, 1993

103 **Mountford C.E.**, Delikatny E J , Dyne M , Holmes K T , Mackinnon W B Ford R , Hunter J C , Truskett I D Russel P Uterine cervical punch biopsy specimens can be analyzed by ^{1}H MRS *Magn Reson Med* , **13**, 324-331, 1990

104 **Le Moyec L.**, Naruse S , Higuchi T , Hirakawa K , Watari H de Certaines J D , Roques H P In vivo ^{31}P MRS in new antineoplastic agents evaluation on experimental tumor models *Cancer Biochem Biophys* , **10**, 31-45, 1988

105 **Narayan P.**, Vigneron D B , Jajodia P , Anderson C M , Hedgcock M W , Tanagho E A , and James T L Transrectal probe for ^{1}H MRI and ^{31}P MR spectroscopy of the prostate gland *Magn Reson Med* , **11**, 209-220, 1989

106 **Narayan P.**, Jajodia P , Kurhanewicz J , Thomas A , MacDonald J , Hubesch B , Hedgcock M , Anderson C M , James T L , Tanagho E A and Weiner M Characterization of prostate cancer, benign prostatic hyperplasia and normal prostates using transrectal ^{31}P magnetic resonance spectroscopy a preliminary report *J Urol* , **146**, 66-74, 1991

107 **Narayan P.** and Kurhanewicz J Mag-

netic resonance spectroscopy in prostate disease diagnostic possibilities and future developments *Prostate Supplment*, **4**, 43-50, 1992

108 **Neil J.L.** The validation of freely diffusible tracer methods with NMR detection for measurement of blood flow *Magn Reson Med* , **19**, 299-304, 1991

109 **Negendank W.G.**, Crowley M G , Ryan J R Keller N A , Evelhoch J L Bone and soft tissue lesions diagnosis with combined H-1 MR imaging and MR spectroscopy in clinical decision making *Radiology*, **172**, 811-815, 1989

110 **Negendank W.G.** Studies of human tumors by MRS a review *NMR Biomed* , **5**, 303-324, 1992

111 **Newell D.R.**, Maxwell R J , Golding B T In vivo and ex vivo magnetic resonance spectroscopy as applied to pharmacokinetic studies with anticancer agents a review *NMR Biomed* , **5**, 273-278, 1992

112 **Ng T.C.**, Evanochko W T , Hiramoto R N et al ^{31}P NMR Spectroscopy of in vivo tumors *J Magn Reson* , **49**, 271-286, 1982

113 **Ng. T.C.**, Vijayakumar S , Majors A W , Thomas F J , Meaney T F , Baldwin N J Response of a non-hodgkin lymphoma to ^{60}C therapy monitored by ^{31}P in situ *Int J Radiat Oncol Biol Phys* , **13**, 1545-1551, 1987

114 **Ng. T.C.**, Grundfest S , Vijayakumar S , Baldwin N J Majors A W , Karalis I Meaney T F , Shin K H , Thomas F J , Tubbs R Therapeutic response of a breast carcinoma monitored by ^{31}P in situ *Magn Reson Med* , **10**, 125-134, 1989

115 **Oberhaensli R.D.**, Bore P J , Rampling R P , Hilton-Jones D Hands L J , Radda G K Biochemical investigation of human tumors in vivo with phosphorus-31 magnetic resonance spectroscopy *Lancet*, **II**, 8-11, 1986

116 **Oberhaensli R.D.**, Rajagopalan B , Taylor D J , Radda G K , Collins J E , Leonard J V , Schwarz H , Herschkowitz N Study of hereditary fructose intolerance by use of ^{31}P nuclear magnetic resonance spectroscopy *Lancet*, **2**, 931-934, 1987

117 **Oberhaensli R.**, Rajagopalan B , Galloway G J , Taylor D J , Rada G K Study of human liver disease with P-31 magnetic resonance spectroscopy *Gut*, **31**, 463-467, 1990

118 **Okunieff P.**, Dols S , Lee J , Singer S , Vaupel P , Neuringer L J , Beshah K Angiogenesis determines blood flow, metabolism, growth rate, and ATPase kinetics of tumors growing in an irradiated bed ^{31}P and ^{2}H nuclear magnetic resonance studies *Cancer Res* , **51**, 3289-3295, 1991

119 **Onodera K.**, Okubo A , Yasumoto K , Susuki T , Kimura G , Nomoto K ^{31}P nuclear magnetic resonance analysis of lung cancer the perchloric acid extract spectrum *Jpn J Cancer Res* , **77**, 1201-1206, 1986

120 **Oosterhof G.O.N.**, Smits G A H J , de Ruyter J E , Schalken J A , Debruyne F M J Effects of high energy shock waves combined with biological response modifiers or adriamycin on a human kidney cancer xenograft *Urol Res* , **18**, 419-424, 1990

121 **Oosterhof G.O.N.**, Smits G A H J , de Ruyter J E , Schalken J A , Debruyne F M J In vivo effects of high energy shock waves on urological tumors, an evaluation of treatment modalities *J Urol* , **144**, 785-789, 1990

122 **Oosterhof G.O.N.** High energy shock waves in urological tumors *Thesis* ISBN 90-9003569-9, 1990

123 **Oosterhof G.O.N.**, Smits G A H J, de Ruyter J E, Schalken J A, Debruyne F M J Effects of high energy shock waves combined with biological response modifiers in different human kidney cancer xenografts *Ultrasound Med Biol*, **17,** 391-399, 1991

124 **Petroff O.A.C.** Spencer D D, Alger J R and Prichard J W High field proton magnetic resonance spectroscopy of human cerebrum obtained during surgery for epilepsy *Neurology*, **39**, 1197 1202, 1989

125 **Pfeiler M.**, Matura E, Ifflander H, Seyler G Lithotripsy of renal and biliary calculi physics, technology, and medical-technical applications *Electromedica*, **57,** 52-63, 1989

126 **Piantini W.**, Sorensen O W and Ernst R P Multiple quantum filters for elucidating NMR coupling networks *Am Chem Soc*, **104**, 6800-6801, 1983

127 **De Potter P.**, von Weymarn C, Zografos L In vivo phosphorus 31 magnetic resonance spectroscopy of human uveal melanomas and other intraocular tumors *Am J Opthalmol*, **111**, 276-288 1991

128 **Prat F.** Ponchon T, Berger F, Chapelon Y, Gagnon P, Cathignol D Hepatic lesions in the rabbit induced by acoustic cavitation *Gastroenterology*, **100,** 1345-1350, 1991

129 **Purcell E.M.**, Torrey H C, Pound R V Resonance absorption by nuclear magnetic moments in a solid *Phys Rev*, **69** 37-38, 1946

130 **Rajagopalan B.**, Blackledge M J, Mc Kenna B J, Bolas N, Radda G K Measurement of phosphocreatine to ATP ratio in normal and diseased human heart by ^{31}P magnetic resonance spectroscopy using the rotating frame depth selection technique *Ann NY Acad Sci* **508**, 321-332, 1987

131 **Randazzo R.F.**, Chaussy C G, Fuchs G J, Bhutta S M, Lovrekovich H, de Kernion J B The in vitro and in vivo effects of extracorporeal shock waves on malignant cells *Urol Res*, **16,** 419-426, 1988

132 **Redmond O.M.**, Stack J P, Dervan P A, Hurson B J, Carney D N, Ennis J T, Osteosarcoma use of MR imaging and MR spectroscopy in clinical decision making *Radiology*, **172**, 811-815, 1989

133 **Redmond O.M.**, Stack J P, O'Connor N G, Codd M B, Ennis J T In vivo phosphorus-31 magnetic resonance spectroscopy of normal and pathological breast tissue *Br J Radiol*, **64** 210 216, 1991

134 **Redmond O.M.**, Stack J P, O'Connor N, Carney D N, Dervan P A, Hurson B J, Ennis J T P-31 MRS as an early prognostic indicator of patient response to chemotherapy *Magn Reson Med*, **25**, 30-44, 1992

135 **Resnick M.I.**, Grayhack J T Treatment of stage IV carcinoma of the prostate *Urol Clin North Am*, 141-161 1978

136 **Rifkin M.D.** Zerhouni E A Gatsonis C A, Quint L E Paushter D M, Epstein J I, Hamper U, Walsh P C, McNeil B J Comparison of magnetic resonance imaging and ultrasonography in staging early prostate cancer *N Engl J Med*, **323**, 621-626, 1990

137 **Rodrigues L.M.**, Midwood C J, Coombes C, Stevens A N, Stubbs M, Griffiths J R ^{31}P-Nuclear magnetic resonance spectroscopy studies of the response of rat mammary tumors to endocrine therapy *Cancer Res*, **48**,

89-93 1988

138 **Ross B.D.**, Radda G K , Gadian D G , Rocker G , Esiri M , Falconer-Smith J Examination of a case of suspected Mc Ardle's syndrome by ^{31}P nuclear magnetic resonance *N Engl J Med* **304**, 1338-1342 1981

139 **Ross B.**, Helsper J T , Cox I J , Young I R , Kempf R Makepeace A , Pennock J Osteosarcoma and other neoplasms of bone Magnetic resonance spectroscopy to monitor therapy *Arch Surg* **122**, 1464-1469 1987

140 **Ross B.D.** Biochemical considerations in ^{1}H spectroscopy Glutamate and glutamine myo-inositol and related metabolites *NMR in Biomed* , **4** 59-63, 1991

141 **Ross B.D.** The biochemistry of living tissues examination by MRS *NMR in Biomed* , **5**, 215, 1992

142 **Ruiz-Cabello J.** and Cohen, J S Phospholipid metabolites as indicators of cancer cel function *NMR in Biomed* , **5**, 226-233, 1992

143 **Russo P.** Heston W D W , Fair W R Suppression of in vitro and in vivo tumor growth by high energy shock waves *Surg Forum*, **36**, 645-648, 1985

144 **Russo P.**, Mies C , Huryk R , Heston W D W, Fair W D Histopathologic and ultrastructural correlates of tumor growth suppression by high energy shock waves *J Urol* **137**, 338-341, 1987

145 **Schiebler M.L.**, Miyamoto K K , White M , Maygarden S L and Mohler J L In vitro high resolution ^{1}H-spectroscopy of the human prostate benign prostatic hyperplasia, normal peripheral zone and adenocarcinoma *Magn Reson Med* , **29**, 285-291 1993

146 **Schick F.**, Bongers H , Kurz S , Jung W-I , Pfeffer M , Lutz O Localized proton MR spectroscopy of citrate in vitro and of the human prostate in vivo at 1 5 T *Magn Reson Med* , **29**, 38-43, 1993

147 **Schnall M.D.**, Lenkinski R E , Pollack H M , Imai Y , Kressel H Y Prostate MR imaging with an transrectal surface coil *Radiology*, **172**, 570-574, 1989

148 **Schnall M.D.**, Lenkinski R E , Milestone B , Ressel H Y *in "Society of Magnetic Resonance in Medicine, ninth annual meeting*, 1990," p 288

149 **Shaka A.J.**, Freeman R J Prepulses for spatial localization *J Magn Reson* , **64**, 145, 1985

150 **McSheehy P.M.**, Griffiths J R ^{19}F MRS studies of fluoropyrimidine chemotherapy A review *NMR Biomed* , **2**, 133-141, 1989

151 **Sijens P.E.**, Wijrdeman H K, Moerland M A , Bakker C J G , Vermeulen J W A H , Luyten P R Human breast cancer in vivo H-1 and P-31 MR spectroscopy at 1 5 T *Radiology*, **169**, 615 620, 1988

152 **Shine N.**, Palladino M A , Patton J S Deisseroth A , Karczmar G S , Matson G B , Weiner M W Early metabolic response to tumor necrosis factor in mouse sarcoma a phosphorus-31 nuclear magnetic resonance study *Cancer Res* , **49**, 2123-2127, 1989

153 **Sillerud L.O.**, Halliday K R , Griffey R H , Fenoglio-Preiser C , Sheppard S In vivo ^{13}C NMR spectroscopy of the human prostate *Magn Reson Med* , **8**, 224-230, 1988

154 **Sillerud L.O.**, Halliday, K R , Freyer, J P , Griffey, R H and Fenoglio-Preiser C ^{13}C and ^{31}P NMR studies of prostate tumor metabolism *Proceedings of the 21st annual Detroit cancer symposium* , Edited by Evelhoch J L , Negendank W , Valeriote F A , Baker L H , 149-179, 1989

155 **Smits G.A.H.J.**, Heerschap A, Oosterhof G O N, Ruijs J H J, Hilberts C W, Debruyne F M J, Schalken J A Early metabolic response to high energy shock waves in a human tumor kidney xenograft monitored by ^{31}P magnetic resonance spectroscopy *Ultrasound Med Biol* **17** 791 801 1991

156 **Smits G.A.H.J.** High energy shock wave induced biological effects in different tumor models *Thesis*, ISBN 90-9004809-X, 1992

157 **Smits G.A.H.J.**, Cornel E B, v d Boogert E Oosterhof G O N Debruyne F M J, Schalken J A, Heerschap A Effects of High energy shock waves on tumor blood flow and metabolism, $^{31}P/^{1}H/^{2}H$ nuclear resonance spectroscopic studies *Submitted*

158 **Smolev J.K.**, Heston W D W, Scott W W, Coffey D S Characterization of the Dunning R 3327H prostatic adenocarcinoma An appropriate animal model for prostatic cancer *Cancer Treat Rep*, **61**, 273-287, 1977

159 **Sostman H.D.**, Charles H C, Rockwell S, Leopold M, Beam C, Madwed D, Dewhirst M, Cofer G, Moore D, Burn R, Oleson J R Soft tissue sarcomas detection of metabolic heterogeneity with P-31 MR spectroscopy *Radiology*, **176**, 837-843, 1990

160 **Steen R.G.**, Tamargo R J, McGovern K A, Rajan S S, Brem H, Wehrle J P, Glickson J D In vivo ^{31}P nuclear magnetic resonance spectroscopy of subcutaneous 9L gliosarcoma effects of tumor and treatment with 1,3 bis(2-chloroethyl)-1 nitrosourea on tumor bioenergetics and histology *Cancer Res*, **48** 676-681, 1988

161 **Steen R.G.**, Response of solid tumors to chemotherapy monitored by in vivo ^{31}P nuclear magnetic resonance spectroscopy a review *Cancer Res*, **49**, 4075-4085, 1989

162 **Steen R.G.**, Edema and tumor perfusion characterization by quantitative ^{1}H MR imaging *AJR*, **158**, 259 264, 1992

163 **Steinbach P.**, Hofstadter F, Nicolai H, Rosslei W, Wieland W In vitro investigations on cellular damage induced by high energy shock waves *Ultrasound Med Biol* **18**, 691-699, 1992

164 **Stone K.R.**, Mickey D D, Wunderli H, Mickey G H, Paulson D F Isolation of a human prostate carcinoma cell line (DU 145) *Int J Cancer*, **21**, 274 281, 1978

165 **Stubbs M.**, Rodrigues L M, Gusterson B A, Griffiths J R Monitoring tumour growth and regression by ^{31}P magnetic resonance spectroscopy *Adv Enzym Regul*, **30**, 217-230, 1990

166 **Thomas M.A.**, Narayan P, Kurhanewicz J, Jajodia P, Weiner M W Titel art *J Magn Reson*, **87**, 610-619 1990

167 **Vaupel P.** Physiological properties of malignant tumours *NMR Biomed*, **5** 220-225, 1992

168 **Vergunst H.**, Terpstra O T, Schroder F H, Matura E Assesment of shock wave pressure profiles in vitro clinical implications *J Lithotripsy & Stone Dis*, **1**, 289-298, 1989

169 **Vigneron D.B.**, Hricah H, James T L, Jajodia P B, Nunes L, Narayan P Androgen sensitivity of rat prostate carcinoma studied by ^{31}P NMR spectroscopy, ^{1}H MR imaging, and ^{23}Na MR imaging *Magn Reson Med*, **11**, 152-160, 1989

170 **Wehrle J.P.**, Li S J, Rajan S S, Steen R G, Glickson J D ^{31}P and ^{1}H NMR Spectroscopy of tumors in vivo, untreated growth and response to

chemotherapy *Ann NY Acad Sci* , **508,** 200-215, 1987

171 **Weiss N.**, Delius M Gambihler S , Dirschedl P , Goetz A , Brendel W Influence of the shock wave application mode on the growth of A-MEL3 and SSK2 tumors in vivo *Ultrasound Med Biol* , **16,** 595-605, 1990

172 **Whitman G.J.R.,** Chance B , Bode H , Maris J , Haselgrove J , Kelley R , Clark B J , Harken A H Diagnosis ad therapeutic evaluation of a pediatric case of cardiomyopathy using phosphorus-31 nuclear magnetic resonance spectroscopy *J Am Coll Cardiol* , **5,** 745-749, 1985

173 **Williams G.R.**, Proctor E , Allen K , Gadian D G , Lockard H A Quantitative estimation of lactate in the brain by ^{1}H NMR *Magn Reson Med* , **7,** 425-431, 1988

174 **Yacoe M.E.**, Sommer G , Pheel D In vitro proton spectroscopy of normal and abnormal prostate *Magn Reson Med* , **19**, 429-438, 1991

CURRICULUM VITAE

Erik Cornel is op 11 september 1964 in Harlingen geboren. In 1982 behaalde hij het diploma Atheneum B aan de RSG Simon Vestdijk te Harlingen.
In september 1982 begon hij met de studie Geneeskunde aan de Rijks Universiteit Groningen. Hij behaalde het doctoraal examen geneeskunde in juli 1987. In december 1989 legde hij met goed gevolg arts examen af.
Van januari 1990 tot en met december 1993 was hij verbonden als wetenschappelijk medewerker aan het Urologisch Research Laboratorium (Hoofd: Dr J.A. Schalken) van de afdeling Urologie (Hoofd: Prof. Dr. F.M.J. Debruyne) van het Academisch Ziekenhuis Nijmegen.
Sedert 1 januari 1994 volgt hij de vooropleiding algemene heelkunde, in het kader van de opleiding tot uroloog, aan de Stichting Deventer Ziekenhuizen te Deventer (opleider: Dr P.J. van Elk).

Stellingen behorend bij het proefschrift

MAGNETIC RESONANCE SPECTROSCOPY IN UROLOGICAL ONCOLOGY

van

E.B. Cornel

1. Magnetische kernspin resonantie spectroscopie (MRS) kan behulpzaam zijn bij de diagnostiek van het adenocarcinoom van de prostaat.

   Dit proefschrift

2. Met behulp van MRS kan een onderscheid gemaakt worden tussen prostaatcarcinomen met verschillend biologisch gedrag.

   Dit proefschrift

3. De anti-proliferatieve werking van hoog-energetische schokgolven (HESG) berust voornamelijk op een tijdelijke vermindering van de doorbloeding van de tumor.

   Dit proefschrift

4. De met HESG samenhangende daling van de tumor weefsel pH wordt voornamelijk veroorzaakt door een verhoogde melkzuursynthese.

   Dit proefschrift.

5. De intra-tumorale concentratie van systemisch gegegeven TNF-α kan drievoudig verhoogd worden door een lokale behandeling met HESG.

   Cornel et al., submitted

6. Het anti-tumor effect van BCG berust op een lokale werking en niet op een specifieke immunologische.

   Cornel et al. J Urol., 149, 179-182, 1993
   Ratliff et al. J Urol., 150, 1018-1023, 1993

7. Het ontbreken van een effectieve fraudebestrijding aan de Nederlandse universiteiten devalueert de waarde van de doctorandus graad.

8. De kosten ten behoeve van de volksgezondheid in Nederland zullen blijven stijgen welke maatregelen de overheid ook neemt. (Baumol's disease) Dientengevolge zullen wijzigingen in het financieringssysteem deze groei alleen marginaal kunnen beinvloeden.

9. Wetenschap is meten wat meetbaar is, en wat niet meetbaar is meetbaar maken.

   Gallilei

10. Zelfs de beste stelling houdt niet altijd stand.